THERMODYNAMIC ANALYSIS OF STEAM ASSISTED CONVERSION OF BIO OIL COMPONENTS TO SYNTHESIS GAS

by

Seda Aktaş

B.S. in Chemical Engineering, Boğaziçi University, 2006

Submitted to the Institute for Graduate Studies in
Science and Engineering in partial fulfillment of
the requirements for the degree of
Master of Science

Graduate Program in Chemical Engineering
Boğaziçi University
2008

THERMODYNAMIC ANALYSIS OF STEAM ASSISTED CONVERSION OF BIO OIL COMPONENTS TO SYNTHESIS GAS

APPROVED BY:

Asst. Prof. Ahmet Kerim Avcı (Thesis Supervisor)	……...
Assoc. Prof. Hasan Bedir	……...
Assoc. Prof. Ramazan Yıldırım	……...

DATE OF APPROVAL: 10.07.2008

ACKNOWLEDGEMENT

First of all, I want to thank my supervisor Asst. Prof. Ahmet Kerim Avcı for guiding me all through this research and encouraging me for further improvements in all steps.

Next, I also thank Assoc. Prof. Hasan Bedir and Assoc. Prof. Ramazan Yıldırım for their kind attendance to my thesis defense.

I am also grateful to Mustafa Karakaya for the answers he provided whenever I need.

I feel deeply grateful to Çiğdem Filiz, Dicle Hasdemir and Fidan Sümbül for the hours we spend together, not only for academic reasons but also for friendship.

I believe I could not complete this thesis without the priceless support of my friends İrem Koçak and Yücel Altuğ, who continue to believe in me every time and every situation.

Last, but not the least, I want to express my deepest gratitude to my family for the endless support they provided throughout my life.

ABSTRACT

THERMODYNAMIC ANALYSIS OF STEAM ASSISTED CONVERSION OF BIO OIL COMPONENTS TO SYNTHESIS GAS

Steam reforming is a well-established route for hydrogen production, but the processing of fossil-based hydrocarbons leads to the generation of carbon dioxide, a well-known greenhouse gas. Recently, the use of biomass-driven resources such as bio-oil has been recognized as a viable solution in terms of its sustainability and its CO_2 neutral behavior. The aim of this study is to investigate the thermodynamics of steam assisted conversions of model components of bio-oil – formic acid, isopropyl alcohol, lactic acid and phenol – and to understand the effect of process variables such as temperature, pressure and inlet steam-to-fuel ratio on the product distribution. For this purpose, a thermodynamic analysis is performed at ranges of temperature, pressure and steam-to-fuel ratio of 600–1000 K, 1–30 bar and 4–9, respectively. The number of moles of each component in the product stream at equilibrium is calculated via the method of Gibbs Free Energy (GFE) minimization technique. The resulting optimization problems are solved using Sequential Quadratic Programming (SQP) algorithm under General Algebraic Modeling System (GAMS) environment. The results indicate that, for all model hydrocarbons and operating conditions, almost complete conversion to H_2, CO, CO_2 and CH_4 are achieved. Temperature and steam-to-fuel ratio have positive effects in increasing hydrogen content of the product mixture at different magnitudes, whereas the increase in pressure suppressed hydrogen production. These trends provide insight about the reaction mechanism and indicate the existence of water-gas shift, methanation and methane steam reforming as major side reactions running parallel to steam reforming of the model hydrocarbon.

ÖZET

BİO YAĞ BİLEŞEN MADDELERİNİN BUHAR İLE SENTEZ GAZLARINA DÖNÜŞÜMLERİNİN TERMODİNAMİK ANALİZİ

Hidrojen üretiminde en yaygın süreç fosil yakıt bazlı hidrokarbonların buhar ile reformlanmasıdır. Ancak fosil yakıtların kullanımı sera gazı etkisini arttıran karbon dioksitin yüksek miktarda üretimine neden olmaktadır. Buna karşılık biyolojik içerikli yakıtlar, sürdürülebilirlik ve doğal karbon dioksit dengesi özellikleri ile bu soruna en yakın çözüm olarak görülmektedir. Bu çalışmanın amacı, biyo-yağ bileşen maddelerin – formik asit, isopropil alkol, laktik asit ve fenol – buhar ile dönüşümlerinin termodinamik analizlerini yapmak ve süreç değişkenleri olan sıcaklık, buhar-yakıt oranı ve basıncın ürün dağılımı üzerindeki etkisini incelemektir. Bu amaçla, sıcaklık, basınç ve buhar-yakıt oranı sırasıyla, 600–1000 K, 1–30 bar ve 4–9 aralığında değişen değerlerde termodinamik analizler yapılmıştır. Gibbs Serbest Enerji minimizasyonu yöntemi ile ürünlerin denge durumundaki mol sayıları belirlenmiştir. Oluşan optimizasyon problemi ardışık karesel programlama algoritması ile çalışan 'General Algebraic Modeling System' (GAMS) ortamında çözülmüştür. Sonuçlar incelendiğinde, model hidrokarbonların tüm analiz koşullarında hemen hemen tamamının ürüne dönüşümü gözlenmiştir. Sıcaklık ve buhar-yakıt oranının ürün dağılımdaki hidrojen oranı üzerinde farklı oranlarda olumlu etkisi olurken, buna rağmen basınçtaki artışın hidrojen üretimini engellediği görülmüştür. Bu eğilimler reaksiyon mekanizmaları hakkında fikir vermiş ve yakıtların buhar ile refromlanmasının yanı sıra önemli oranda su–buhar dengesi, metanın buhar ile reformlanması ve metanlaştırma reaksiyonlarının varlığını işaret etmiştir.

TABLE OF CONTENTS

ACKNOWLEDGEMENT iii
ABSTRACT iv
ÖZET v
LIST OF FIGURES viii
LIST OF TABLES x
LIST OF SYMBOLS/ABBREVIATIONS xii
1. INTRODUCTION 1
2. LITERATURE SURVEY 5
2.1. Steam Reforming of Light Hydrocarbons 5
2.1.1. Methane Steam Reforming 6
2.1.2. Methanol Steam Reforming 8
2.1.3. LPG and Dimethyl Ether Steam Reforming 9
2.2. Steam Reforming of Biofuels 11
2.2.1. Ethanol Steam Reforming 13
2.2.2. Glycerol Steam Reforming 15
2.2.3. Ethylene Glycol Steam Reforming 17
2.2.4. Acetic Acid Steam Reforming 19
2.2.5. Acetone Steam Reforming 20
2.2.6. Phenol Steam Reforming 21
2.2.7. 2-propanol Steam Reforming 22
2.3. Deterministic Optimization Techniques 22
3. MATHEMATICAL TECHNIQUES FOR THE PREDICTION OF CHEMICAL REACTION EQUILIBRIUM 25
3.1. Introduction to Mathematical Techniques for Chemical Equilibrium 25
3.2. Mathematical formulation of the Gibbs Free Energy Minimization 26
3.2.1. Mathematical Formulation for Ideal Gas Model 27
3.2.2. Mathematical Formulation for Non Ideal Gas Model 28
3.2.3. Elemental and Feasibility Constraints 31
3.3. Optimization via Sequential Quadratic Programming 32
3.4. Application of SQP to Solution of GFE Minimization Problems 34

4. RESULTS AND DISCUSSION 36
4.1. Results of Thermodynamic Analysis at 1 bar 36
4.1.1. Formic Acid 37
4.1.2. Isopropyl Alcohol 39
4.1.3. Lactic Acid 41
4.1.4. Phenol 43
4.2. Results of Thermodynamic Analysis at 30 bar 45
4.2.1. Formic Acid 45
4.2.2. Isopropyl Alcohol 48
4.2.3. Lactic Acid 50
4.2.4. Phenol 51
5. CONCLUSIONS AND RECOMMENDATIONS 54
5.1. Conclusions 54
5.2. Recommendations 55
APPENDIX 56
REFERENCES 58

LIST OF FIGURES

Figure 2.1. Flow diagram of production of synthetic diesel from biomass via steam reforming of bio-oil 12

Figure 3.1. General optimization problem for SNOPT algorith 12

Figure 4.1. Effects of temperature and steam to fuel ratio on the mole fractions of the products during Formic Acid conversion (dry basis, 1 bar) (a) H_2, (b) CO, (c) CO_2, (d) CH_4 38

Figure 4.2. Effects of temperature and steam to fuel ratio on the mole fractions of the products during Isopropyl Alcohol conversion (dry basis, 1 bar) (a) H_2, (b) CO, (c) CO_2, (d) CH_4 40

Figure 4.3. Effects of temperature and steam to fuel ratio on the mole fractions of the products during Lactic Acid conversion (dry basis, 1 bar) (a) H_2, (b) CO, (c) CO_2, (d) CH_4 42

Figure 4.4. Effects of temperature and steam to fuel ratio on the mole fractions of the products during Phenol conversion (dry basis, 1 bar) (a) H_2, (b) CO, (c) CO_2, (d) CH_4 44

Figure 4.5. Effects of temperature and steam to fuel ratio on the mole fractions of the products during Formic Acid conversion (dry basis, 30 bar) (a) H_2, (b) CO, (c) CO_2, (d) CH_4 47

Figure 4.6. Effects of temperature and steam to fuel ratio on the mole fractions of the products during Isopropyl Alcohol conversion (dry basis, 30 bar) (a) H_2, (b) CO, (c) CO_2, (d) CH_4 49

Figure 4.7. Effects of temperature and steam to fuel ratio on the mole fractions

of the products during Lactic Acid conversion (dry basis, 30 bar)
(a) H_2, (b) CO, (c) CO_2, (d) CH_4 51

Figure 4.8. Effects of temperature and steam to fuel ratio on the mole fractions
of the products during Phenol conversion (dry basis, 30 bar)
(a) H_2, (b) CO, (c) CO_2, (d) CH_4 52

LIST OF TABLES

Table 3.1. Equations of the ideal modeled optimization (Sandler, 1989; Floudas, 2000) 28

Table 3.2. Equations of the non ideal modeled optimization (Harding and Floudas, 2000)..... 30

Table 3.3. SQP results under different z boundaries (phenol steam reforming at 30 bar) 35

Table 4.1. Deviations of the mole fractions of the products of Formic Acid conversion from 1 bar to 30 bar (dry-basis) 46

Table 4.2. Deviations of the mole fractions of the products of Isopropyl Alcohol conversion from 1 bar to 30 bar (dry-basis)..... 48

Table 4.3. Deviations of the mole fractions of the products of Lactic Acid conversion from 1 bar to 30 bar (dry-basis) 50

Table 4.4. Deviations of the mole fractions of the products of Phenol conversion from 1 bar to 30 bar (dry-basis) 52

Table 4.5. Number of moles and compressibility factors obtained for steam reforming of phenol at 30 bar 53

Table A.1. Gibbs free energy of formation (J/mol) of selected hydrocarbons (CRC Handbook, 1985)..... 56

Table A.2. Gibbs free energy of formation (J/mol) of products (CRC Handbook, 1985)..... 56

Table A.3. Gibbs free energy of formation (J/mol) of possible hydrocarbon-based side products (CRC Handbook, 1985)..... 56

Table A.4. Thermodynamic critical constants of selected hydrocarbons (Reid et al.,c1987)..... 57

LIST OF SYMBOLS/ABBREVIATIONS

a_{ei}	Number of element (e) in component (i)
A_i	SRK Parameter
$A_{i,j}$	SRK interaction Parameter in mixture
A^{mix}	SRK Parameter in mixture
b_e	Number of element (e) at equilibrium
B_i	SRK Parameter
B^{mix}	SRK Parameter in mixture
d_k	Search direction in SQP
$\hat{f}_i$	Fugacity of pure component
f_i^0	Fugacity of pure component at ideal state
$\overline{G}_i$	Chemical Potential
$G_{i,f}^0$	Gibbs Free Energy of Formation at 298 K 1 bar
G_t	Total Gibbs Free Energy
H_k	Approximation of the Hessian
$k_{i,j}$	Interaction Parameter
L	Lagrangian Function
m_i	SRK parameter
n_i	Number of moles
n_t	Total Number of Moles
P_c	Critical Pressure
P	System Pressure
R	Universal Gas Constant
T	Temperature
T_c	Critical Temperature
w	Acentric Factor
x_i	Mole Fraction

x_k	Approximation of the Solution in SQP
z	Compresibility Factor
$\hat{\phi}$	Fugacity coefficient of pure component
ω	Excess variable to prevent the division by zero condition
ΔH^0_{298}	Enthalpy of Reaction
α	Excess variable to diminish the nonlinearity
α_k	Step Length Parameter
λ_k	Approximation of the Multiplier in SQP

EOS	Equation of State
GAMS	General Algebraic Modeling System
GFE	Gibbs Free Energy
LPG	Liquefied Petroleum Gas
QP	Quadratic Programming
RWGS	Reverse Water Gas Shift
S/C	Steam to Carbon
S/F	Steam to Fuel
SMR	Steam Methane Reforming
SR	Steam Reforming
SRK	Soave-Redling-Kwong
WGS	Water Gas Shift

1. INTRODUCTION

Synthesis gas is a mixture of carbon monoxide and hydrogen and is used in chemical process industries as a feedstock in the production of commodities such as methanol and ammonia (Balasubramanian *et al.,* 1999). The conventional route of synthesis gas production is via catalytic steam reforming of hydrocarbon fuels, and, in most cases, natural gas (Mohanty, 2006). In this process, the hydrocarbon fuel is reformed into a mixture of carbon monoxide, carbon dioxide and hydrogen in the presence of steam and a catalyst (Ni based) at high temperatures (ca. 800°C), (Balasubramanian *et al.,* 1999; Barelli *et al*., 2008). Steam reforming (SR) is a well-established route, but the processing of fossil-based hydrocarbons in it leads to the generation of carbon dioxide, a well-known greenhouse gas. When this is combined with the increased rate of depletion of fossil fuels, use of alternative resources such as biomass-based feedstocks; ethanol (Yang *et al*., 2006), ethylene glycol (Luo *et al*., 2007), acetic acid (Bimbela *et al*., 2000; Rioche *et al*., 2005; Takanabe, *et al*., 2004), dimethyl ether (Faungnawakij *et al*., 2006) started to receive significant interest. Biomass has been recognized as viable solutions being renewable, abundant and practical energy resource with its CO_2 neutral energy conversion, ease of storage and transportation. (Resini *et al*., 2006; Basagiannis and Verykios, 2007).

The conversion of biomass-based feedstocks to synthesis gas can be achieved either by its direct gasification or by its pyrolysis to a liquid substance called bio-oil followed-up by steam reforming of bio-oil (Basagiannis and Verykios, 2007; Bimbela *et al*., 2000; Ni *et al*., 2006). The former process, biomass gasification, involves complex reactions, such as pyrolysis, hydrolysis, steam reforming, water–gas shift (WGS) reaction and methanation (Yan *et al*., 2006) resulting a mixture of gases (mainly consisting of H_2, CO, CO_2, CH_4 and higher hydrocarbons), solids (char) and liquids (aromatic hydrocarbons) known as ‘tars’. Steam, air and CO_2 are some examples of the gasifying agents. The product distribution highly depends upon the operating conditions in addition to biomass type, physical characteristics of biomass and the gasifier design (Mahishia and Goswamib, 2007).

The second route involves two steps: In the first step, pyrolysis takes place to convert the biomass, via heating it 650 – 800 K at 0.1–0.5 MPa in the absence of air (Ni *et al*.,

2006). Depending on pyrolysis conditions different product distributions are observed including groups of acids, alcohols, aldehydes, esters, ketones, sugars and phenols (Basagiannis and Verykios, 2007). Pyrolysis product gases are then produced in the second step by steam reforming of the bio-oil. The unwanted tar may cause the formation of tar aerosols and polymerization to a more complex structure, which are not favorable for hydrogen production through steam reforming (Ni *et al*., 2006) and diversification of the gasification compounds is also difficult. Their reforming also include aromatic ring, such as coal tar or lignin derived aromatics which leads to carbon deposition on the catalyst thus the direct gasification is not favorable due to these circumstances (Ishihara *et al*., 2005).

Bio-oil is defined as a mixture of a variety of aliphatic and aromatic oxygenates such as aldehydes, ketones, acids and alcohols, with the exact composition being determined by the type and the origin of the biomass feedstock (Rioche *et al*., 2005). The components of bio-oil are usually complex and, therefore, simpler model compounds such as acetic acid, ethylene glycol, acetone (Vagia and Lemonidou, 2007), glycerol (Adhikari *et al*., 2007), cresol (Iojoiu *et al*., 1997), benzene (Simell *et al*., 2004) are employed to represent it.

In recent years, steam reforming conversion of model compounds of bio-oil are studied experimentally and theoretically. Experimental studies involve various model compounds focusing different objectives. Bimbela and coworkers (2000) have carried out an experimental study taking acetic acid as model compound and analyzed hydrogen yield with three different catalysis at various temperatures. Similarly, Marquevich and coworkers (1999) conducted experiments including three compounds representing also different groups of model hydrocarbons, m-cresol, dibenzyl ether, glucose, xylose, and sucrose at different gas hourly space velocities changing steam-to-carbon ratios from 3 to 6 and catalyst temperatures from 550 to 810°C. Besides the hydrogen yield calculations, coking and decomposition of some components are observed. In another study, toluene steam reforming is examined with Ni/olivine catalyst between 560 - 850°C and a kinetic model is established in which the kinetic parameters are found to be comparable to benzene or tars (Swierczynski *et al*., 2008).

Thermodynamic analysis of the bio-oil conversion process compose the theoretical group of studies and involve a set of calculations to predict the molar composition of a

mixture at its thermodynamic equilibrium at the specified state properties and help to understand the effects of operating conditions such as temperature, pressure and inlet compositions on the product distribution. Such studies are used to obtain a direction for the actual operating conditions that will yield the desired product distribution window. Previously, acetic acid (Vagia and Lemonidou, 2007), ethylene (Luo *et al*., 2007), glycerol (Adhikari *et al*, 2007) have been analyzed as the model compound of bio oil steam reforming studies via different techniques.

Mathematical solution of thermodynamic equilibrium of a reactive system can be done either via solving the multi-reaction equilibria equations or via minimizing the total Gibbs Free Energy of the system (Floudas, 1997). In first method, system is described by stoichiometrically independent reactions (Mas *et al*., 2006) that are selected form a set of possible reactions (Fishtik *et al*., 2000; Adhikari *et al*., 2007) and requires the knowledge of reaction mechanism. Equilibrium concentrations are then obtained through solving the non-linear equations including heat of reactions, equilibrium constant and equilibrium molar fractions of components (Luo *et al*., 2007). On the other hand, second technique is usually preferred as it can estimate the equilibrium compositions when unclear reaction mechanisms are examined in which information sets about reaction mechanism are scarce (Mas *et al*., 2006; Yan *et al*., 2006) and only possible components at equilibrium conditions are required (Floudas, 1997). This knowledge is inserted into the mathematical formulation of the Gibbs free energy and resulting model produces an optimization problem. Gibbs free energy minimization problem is generally solved by Lagrange's multiplier method satisfying the elemental mass balances (Adhikari *et al*., 2007; Faungnawakij *et al*., 2006; Mahishia and Goswamib, 2007). In addition, direct minimization methods including deterministic mathematical tools for nonlinear object function minimization are also applied for single phase or multiphase calculations of the minimum Gibbs free energy (Faungnawakij *et al*., 2006). On the other hand, recently there are also probabilistic approaches in determination of the phase equilibrium and component distribution. Rangaiah (2006) has applied genetic algorithms in the phase equilibrium and stability calculations. These algorithms have also been used for the estimation of kinetic parameters (Harris *et al*., 2000; Mansoornejad *et al*., 2008; Elliott *et al*, 2000).

The objective of this study is to explore the thermodynamics of steam assisted conversion of bio-oil compounds – formic acid, isopropyl alcohol, lactic acid and phenol – to synthesis gas using Gibbs free energy minimization technique. The effects of operating temperature, pressure and the inlet steam/fuel ratio, at ranges of 600-1000 K, 1-30 bar and 4-9, respectively, on the molar distribution of the reactant and product species are investigated. The operating ranges have been selected to cover both ideal and non-ideal gas behaviors. Mathematical solutions of the optimization problems are executed using the deterministic Sequential Quadratic Programming method.

The literature survey presented in Chapter 2 is about both steam reforming process of hydrocarbons (renewable and non-renewable) and deterministic optimization algorithms. The mathematical techniques of the thermodynamic analysis are given in the first part of Chapter 3 while the model equations that are used in this study are given in latter part of the this chapter. Chapter 4 is devoted to the statement of both the results calculations and the discussions results of calculations. Thesis ends with Chapter 5, which states the major outcomes of this study and the recommendations for the future work.

2. LITERATURE SURVEY

2.1. Steam Reforming of Light Hydrocarbons

The conventional method of producing hydrogen or synthesis gas – a mixture of hydrogen, carbon monoxide and carbon dioxide – is by steam reforming of hydrocarbons. Steam reforming (SR) (Reaction (2.1)) is a catalytic reaction, in which hydrogen is extracted from the feed hydrocarbon and steam at temperatures higher than ca. 500°C (Rostrup-Nielsen, 1984). The outlet mixture of the reaction, called synthesis gas (syngas), is either purified to hydrogen for meeting the hydrogen demands in refineries or is directly used as a feedstock in processes such as methanol and ammonia synthesis and in production of synthetic fuels via the Fisher-Tropsch mechanism (Barelli *et al*., 2008).

$$CH_4 + H_2O = CO + 3H_2 \qquad \Delta H^0_{298} = 206.2 \text{ kJ/gmol} \quad (2.1)$$

$$CO + H_2O = CO_2 + H_2 \qquad \Delta H^0_{298} = -41.2 \text{ kJ/gmol} \quad (2.2)$$

Steam reforming is endothermic and is thermodynamically favored at high temperatures with low pressures and considerable heat should be supplied from the surroundings (Rostrup-Nielsen, 1984). An important side reaction, water–gas shift (WGS) (Reaction 2.2), takes place simultaneously with the SR reactions independently. In most cases, this reaction is run separately at the downstream to adjust the hydrogen-to-carbon monoxide ratio of the synthesis gas to a value suitable for the post-synthesis application of interest. Most of these applications, such as methanol synthesis, are favored thermodynamically at pressures greater than 20 bars. Therefore, in industrial practice, the steam reforming processes are carried out at high pressures (Armor, 1999). Natural gas and naphtha are the commonly used fuels in conventional steam reforming processes (Basagiannis and Verykios, 2007).

Steam reforming of hydrocarbons is catalyzed mostly by the Ni-based catalysts (Joensen and Rostrup–Nielsen, 2002). It is well known that, in addition to the nature of the

catalyst and its composition, the operating conditions have significant effects on product distribution and the stability of the operation. In general, steam-to-fuel (S/F) ratio, operating temperature (T) and pressure (P) appear to be the main process variables that dictate the product distribution and critical limits of the catalyst deactivation. Therefore, in order to obtain a desired product specification, it is necessary to know the effect of these variables on the product distribution. Usually, the first step to understand the qualitative and quantitative effects of the operating conditions is to conduct a thermodynamic analysis for the particular conversion process (Fishtik *et al*., 2000).

Thermodynamic analysis of a chemically reacting system is used in predicting the product distribution at a given temperature and pressure when there are no detailed kinetic information about the reacting systems such as reaction expression or stochiometric data (Floudas, 1997). This methodology can be used in characterizing, understanding and designing reaction systems to meet the design objectives such as maximizing reactant conversion or selectivity of a desired product. Thermodynamic analysis can be conducted via two methods: simultaneous solution of the reaction equilibrium equations and minimization of Gibbs Free Energy (GFE) of the system at specified temperature and pressure (Floudas, 2000).

2.1.1. Methane Steam Reforming

Hydrogen is widely produced from natural gas, consisting considerable amount of methane, via steam methane reforming (SMR) (Vagia and Lemonidou, 2007). SMR is normally carried out at a temperature range of 800–1000°C and a pressure range of 15 – 30 bar over supported nickel-based catalyst packed in multiple parallel tubular, externally heated reactors (Barelli *et al*., 2008). This process is limited by thermodynamic equilibrium of the reversible reactions, high-energy demand, severe reaction conditions (due to presence of high temperatures, pressures and steam, the latter which facilitates the corrosion of materials of construction), catalyst deactivation (mainly due to sintering and carbon formation) and increased CO_2 emissions (Barelli *et al*., 2008).

Since SMR is a conventional process, recent studies focus on catalyst improvement or energy enhancement of the process rather than the operation conditions. However the

studies characterizing the SMR reaction conditions are important guides for designing further experiments in such a way that more useful data could be collected (Seo *et al*, 2002). Therefore the objective of some the recent studies is to calculate the maximum allowable hydrogen yield with minimum carbon monoxide and solid carbon, $C_{(s)}$, production by figuring out the optimal combinations of operating temperature, pressure and the inlet steam-to-fuel ratio (Joensen and Rostrup–Nielsen, 2002).

Reactor temperature has an important effect on equilibrium compositions and feed conversions during methane steam reforming. Results observed from various studies clearly indicates that hydrogen production and methane conversion are substantial at temperatures higher than 400°C and, when the temperature is increased from 600°C to 800°C, methane conversion changes from 0.56 to 0.90 (Seo *et al*, 2002). This behavior is in alignment with the thermodynamics, in which the equilibrium CH_4 conversion is 0.99 at 700°C, which is encountered in all studies (Rakass *et al.*, 2006). The increase in temperature from 400°C to 700°C gradually promotes the formation of CO and CO_2 together with the increase in H_2 production. Further increase of temperature in excess of 800°C can maximize methane conversion, but thermal deactivation of the catalyst due to sintering and carbon formation due to methane cracking may become significant (Rakass *et al.*, 2006).

Methane conversion and carbon formation is also strongly affected by the steam-to-carbon ratio (S/C) at the inlet. It is observed that at 600°C methane conversion changes from 0.60 to 0.75 as the S/C is increased from 1.5 to 2.5. It is also reported that S/C higher than 2.5 is required for achieving methane conversion near 95 per cent at 700°C while at temperatures higher than 800°C, S/C ratios just above 1.2 gives conversion values greater than 0.95 (Seo *et al.*, 2002). It is clear that S/C affects the product distribution, so different ranges upon the aim of study are investigated for hydrogen production system. Rakass and coworkers (2006) performed experiments involving range of steam-to-fuel ratio and temperature between 0.5 – 2.0 and 100 – 700°C, respectively. At higher steam-to-fuel ratios, carbon deposition is observed to diminish steam reforming of methane dominates the reforming system and the excess steam enhances the carbon gasification which suppresses the carbon deposition on the nickel reforming catalyst. Thermodynamic

simulations indicate that a steam-to-fuel ratio of 2 and temperatures near 700°C provide favorable operating conditions (Rakass *et al.*, 2006).

Pressure is another parameter affecting product distribution during methane steam reforming. As pressure is increased, methane conversion, production of H_2 and CO is decreased due to stoichiometric relation of the SMR. The number of moles in the products is higher and the increased pressure shifts the equilibrium to reactants due to Le Chatelier principle to lower the volume. Therefore favorable operating conditions can be ensured with proper combination of temperature, pressure and S/C ratio. Optimum ratio of S/C is suggested as 1.9 or higher, with over 800°C under low pressures (Seo *et al.*, 2002).

2.1.2. Methanol Steam Reforming

Steam reforming of methanol is an attractive alternative for small hydrogen plants and for hydrogen generation in fuel cell driven transportation concepts. This reaction is less endothermic relative to methane steam reforming and almost 99 per cent conversion can be reached at 200–300°C:

$$CH_3OH + H_2O = CO_2 + 3H_2 \qquad \Delta H^0_{298} = 49.5 \text{ kJ/mol} \quad (2.3)$$

$$CH_3OH = CO + 2H_2 \qquad \Delta H^0_{298} = 90.7 \text{ kJ/mol} \quad (2.4)$$

Methanol steam reforming involves a complex reaction system and the purity of hydrogen product can be affected by many undesirable side reactions (Fishtik *et al.*, 2000). The plausible product distribution changes but one of the most expanded distribution may include; methane, carbon (graphite), methane, ethane, propane, i–butane, n–butane, ethanol, propanol, i–butanol, n-butanol and dimethyl ether (Faungnawakij *et al.*, 2006).

Thermodynamic analysis of methanol steam reforming is conducted between 360 and 573 K and assuming at 1 atm, at a steam to methanol ratio range of 0 to 1.5 (Lwin *et al.*, 2000). Faungnawakij and co-workers (2006) studied methanol steam reforming at a temperature range of 25–1000°C with steam to carbon ratio between 0 and 10 and pressure

between 0.5 and 3 atm. Thermodynamic equilibrium products include high H_2 and low CO at temperatures around 400-460 K. Temperatures higher than 450 K results in decrease H_2 production and less favored WGS leaves unreacted H_2O (Lwin *et al*., 2000). The RWGS expedites the consumption of hydrogen, and is thermodynamically favorable with increasing temperature (Faungnawakij *et al*., 2006).

The comprehensive thermodynamic analysis of methanol steam reforming performed by Faungnawakij and co-workers (2006) show that complete methanol conversion is obtained at S/C of 2 and at 100°C. Hydrogen yield is obtained as 73.2 per cent which is very similar to the 75 per cent showing the theoretical hydrogen mole percent at T=150°C, S/C=1. Further increase in temperature elevates methanol conversion, but also leads to a decrease in hydrogen mole fraction due to the dominance of the RWGS consuming H_2. S/C ratios lower than 1.5 is found to lead to higher CO concentrations, which is reported to be a source of coke formation over steam reforming catalysts. However, at temperatures lower than 150°C, the conversion was suppresses by increasing pressure (Faungnawakij *et al.*, 2006).

2.1.3. LPG and Dimethyl Ether Steam Reforming

Apart from methane and methanol, other hydrocarbons such as LPG (Liquefied Petroleum Gas) and dimethyl ether are also investigated for their conversion to synthesis gas and hydrogen for use in fuel cell applications (Avcı *et al.*, 2001, 2004; Semelsberger and Borup, 2005). In case of such higher hydrocarbons, rates of steam reforming over a particular catalyst can be faster than that of methane, but non-catalytic thermal cracking reactions can be significant enough to compete with the catalytic ones at temperatures over 600–650°C to lead to coke formation and catalyst deactivation (Joensen and Rostrup–Nielsen, 2002).

LPG is a mixture of propane and n-butane in ranges from pure propane to a 40:60 mixture of propane and n-butane. The main products from the steam reforming of LPG are hydrogen, carbon monoxide, and carbon dioxide, however, the formation of ethane, ethylene, and methane are usually observed due to the decomposition of LPG and methanation reactions (Laosiripojana and Assabumrungrat, 2006).

The studies considering temperature interval of 700–900°C and steam-to-LPG ratio range of 3–7 under atmospheric pressure show that at high temperatures such as 900°C, the main products from the steam reforming reaction are CH_4, H_2 CO, CO_2 and trace amounts of C_2H_4. Hydrogen and carbon monoxide selectivity increases with increasing temperature, whereas carbon dioxide and ethylene production selectivity decreases. These changes in product selectivity are mainly due to the influence of the exothermic water–gas shift reaction, whereas the decreased methane and ethylene selectivity could be due to further reforming which would generate more carbon monoxide and hydrogen (Laosiripojana and Assabumrungrat, 2006).

Dimethyl ether is an alternative fuel for renewable energy sources with low reforming temperatures and complete conversion to H_2, CO and CO_2. Besides the ease of storage, handling and low NO_x, SO_x, and particulate matter emissions, it has also been used in industry as refrigerant and diesel substitute and additive (Semelsberger and Borup, 2005).

Semelsberger and coworkers (2005) investigated the optimum thermodynamic parameters of dimethyl ether steam reforming in a temperature range of 100–600°C pressure range of 1-5 atm and steam-to-carbon range of 0.5–4. Thermodynamic analysis is performed using Gibbs free energy minimization with a Lagrange multiplier optimization method with expanded product set additional to conventional syngas components. The equation of state used was the Peng–Robinson equation. Minimization was accomplished with Aspen Tech^{TM}, commercial software capable of performing multicomponent equilibria. In all cases, the product sets did not include carbon as a thermodynamically viable species. The results show that steam reforming conversion of dimethyl ether is not limited by equilibrium and reaches to 1 for the whole operating range. The composite reaction was taken as the product basis set (CH_3OCH_3, H_2O, CO_2, CO, H_2) with steam–to–carbon ratios ranging from 0 to 4 for simulations and (Semelsberger and Borup, 2005).

Further results are discussed based on a hydrogen efficiency parameter which is defined as the mole fraction of the hydrogen in wet basis divided by the theoretical mole fraction of hydrogen in steam reforming whose value is taken as 0.75. It is observed that as steam–to–carbon ratio is increased, hydrogen efficiency is decreased due to the steam

dilution. At a constant steam–to–carbon ratio and at increasing temperatures, mole fractions of hydrogen and carbon monoxide are found to decrease and increase, respectively primarily due to the water–gas shift equilibrium. The hydrogen mole fraction increases with increasing steam–to–carbon ratio because of the increased conversion of dimethyl ether to hydrogen, reaching a maximum at a steam–to–carbon ratio of 1.50, then decreases as the steam–to–carbon ratio is further increased because of steam dilution. The hydrogen mole fraction on a wet basis decreases faster due to steam dilution than the increase in hydrogen production from the water–gas shift reaction as the steam–to–carbon ratio is increased.

The optimal steam–to–carbon ratio of 2.50 was chosen to investigate the effects of pressure on dimethyl ether steam reforming and determine the thermodynamically viable products during the process of dimethyl ether steam reforming. It is observed that increasing the pressure from 1 to 5 atm decreases the hydrogen production efficiency by 12 per cent and decreases dimethyl ether conversion by 23 per cent. Increasing the pressure shifts the equilibrium to the reactants; hence dimethyl ether steam reforming should be operated at low pressures to maintain a high degree of hydrogen production efficiency (Semelsberger and Borup, 2005). For a constant S/C ratio of 2 and a pressure of 1 atm, thermodynamic equilibrium compositions were simulated for the determination of additional products in the temperatures ranging from 100 to 600°C (Semelsberger and Borup, 2005). It can be noted that, if the catalysts employed are not selective toward hydrogen, carbon monoxide and carbon dioxide, then additional thermodynamically stable products are observed (Semelsberger and Borup, 2005).

2.2. Steam Reforming of Biofuels

Global warming is one of the permanent results of high greenhouse gas emissions caused by widespread use of fossil fuels for energy production. Many studies and improvements are being made on resolving the issue of global warming such as finding sustainable energy conversion technologies and recovery and the disposal of greenhouse gases. Alternative clean energy sources are gaining attention to diminish the effect of fossil fuels. Biomass has been recognized as viable solutions being renewable, abundant and easy to use energy resource with its CO_2 neutral feature (Basagiannis and Verykios, 2007; Ni *et*

al., 2006). Biomass is defined as any hydrocarbon material, which mainly consists of carbon, hydrogen, oxygen and nitrogen. The major organic components of biomass can be classified as cellulose, hemicellulose and lignin (Yaman, 2004).

Hydrogen is produced from biomass via different technical pathways, i.e. anaerobic digestion, fermentation, metabolic processing, high-pressure supercritical conversion, gasification and pyrolysis, in which the latter two appear be viable at the current stage from both economical and technical views (Vagia and Lemonidou, 2007). Using biomass as hydrogen source consists two step processes, first pyrolysis or gasification to produce bio oil and a second step where the bio-oil or a fraction of it is transformed into a gas rich in hydrogen by steam catalytic reforming followed, if necessary, by a water–gas shift conversion step (Bimbela *et al.*, 2000; Ni *et al.*, 2006; Basagiannis and Verykios, 2007). The flow diagram of pyrolysis conversion of biomass into bio-oil followed by its steam reforming for use in hydrocracking to produce synthetic diesel fuel is shown in Figure 2.1.

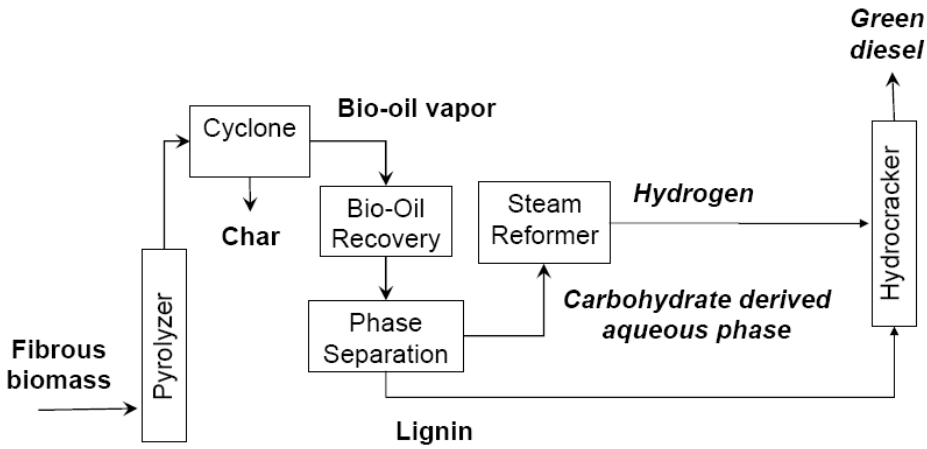

Figure 2.1. Flow diagram of production of synthetic diesel from biomass via steam reforming of bio-oil

The composition of bio-oil varies significantly with the type of biomass and the conditions of pyrolysis. The typical mixture includes low and high molecular weight oxygenated compounds such as carboxylic acids, aldehydes, ketones, esters, sugars, alcohols and phenols (Rioche *et al.*, 2005). This bio-oil can be reformed as a whole or in separated forms. Addition of water to bio-oil splits it up into two immiscible phases: an

aqueous phase containing carbohydrates-derived compounds and some light oxygenated compounds, which can be reformed with steam to hydrogen and the second hydrophobic phase formed mainly by aromatic and lignin derived materials that can be used for the production of more valuable products (Iojoiu *et al.*, 2007; Bimbela *et al.*, 2000).

Key compounds identified are phenols (phenol and cresols), furfurals, acids (acetic acid, formic acid, lactic acids) and aldehydes (acetic aldehyde and formic aldehyde). Steam reforming of hydrocarbon liquids glycerin, ethanol and vegetable oils are studied (Bimbela *et al.*, 2000) and up to now, catalytic steam reforming (SR) of oxygenated compounds such as acetic acid, hydroxy-acetaldehyde, ethanol, acetone, phenol or cresol among others, used as model compounds of bio-oils (Iojoiu *et al.*, 2007)

2.2.1. Ethanol Steam Reforming

Ethanol is an oxygenated hydrocarbon, and has advantage of cheap and easy transportation, safe handling, low toxicity and biodegradability. Steam reforming of ethanol and the associated reaction network can be given as follows (Yang *et al.*, 2006).

$$CH_5OH + 3H_2O = 2CO_2 + 6H_2 \qquad \Delta H^0_{298} = 173.5 \text{ kJ/gmol} \quad (2.5)$$

$$C_2H_5OH = CH_4 + H_2 + CO \qquad \Delta H^0_{298} = 49.5 \text{ kJ/gmol} \quad (2.6)$$

$$CO + 3H_2 = CH_4 + H_2O \qquad \Delta H^0_{298} = 206.2 \text{ kJ /gmol} \quad (2.7)$$

Similar to previous hydrocarbons, ethanol steam reforming is also affected by three main parameters – temperature, pressure and steam-to-fuel ratio. It is observed that increase in the steam-to-fuel ratio improves hydrogen selectivity. In addition the CO_2 content in the effluent stream increases and byproducts such as CO and CH_4 decrease with higher steam-to-fuel ratios. These results are explained with possible reactions such as reforming and shift reactions, Reactions (2.5) and (2.2), respectively, which are favored at higher steam-to-fuel ratios. It was also given that complete conversion of ethanol is obtained in temperature range of 300–650°C (Yang *et al.*, 2006).

Yang and coworkers (2006) have also found that the conversion of steam increased with temperature and remained constant at temperatures above 530°C. Furthermore, the concentration of CO, CO_2 and CH_4 underwent a similar three–stage change (Yang *et al.*, 2006). At temperatures below 380°C, the conversion of ethanol was already close to completion, the conversion of water was about 60 per cent, and the selectivity to hydrogen was less than 60 per cent. On the other hand, the concentration of CO and methane was high and decreased with the increase of temperature, while the concentration of CO_2 increased. These phenomena indicate that at this stage the reforming reaction, Reaction (2.5),and decomposition reaction, Reaction (2.6) predominated; meanwhile, shift reaction ,Reaction (2.2) and methanation reaction, Reaction (2.7) were also involved (Yang *et al.*, 2006).

When temperature is increased to 530°C, the consumption of water reached close to its stoichiometric value and the selectivity increased to over 80 per cent. At the same time, the concentration of methane decreased further, the formation of CO_2 passed through a maximum, and the concentration of CO underwent a minimum. These phenomena imply that besides reforming of ethanol, the reformation of methane (Reactions (2.8) and (2.9)) and the reverse shift reaction, Reaction (2.10) were accelerated:

$$CH_4 + 2H_2O = CO_2 + 4H_2 \qquad \Delta H^0_{298} = 165.1 \text{ kJ/gmol} \quad (2.8)$$

$$CH_4 + CO_2 = 2CO + 2H_2 \qquad \Delta H^o_{298} = 247.4 \text{ kJ/gmol} \quad (2.9)$$

$$CO_2 + H_2 = CO + H_2O \qquad \Delta H^o_{298} = +41.2 \text{ kJ/gmol} \quad (2.10)$$

Ethanol and water was stoichiometrically complete and selectivity to hydrogen increased further with temperature to over 90 per cent at 650°C. The concentration of methane was decreased. However, the content of CO_2 did not recover and correspondingly, the formation of CO increased. Therefore, it can be recognized that the dry reforming reaction, Reaction (2.9), and the reverse shift reaction, Reaction (2.10), were accelerated in this stage, although the steam reforming of methane was also promoted at a high temperature.

The concentration of CO_2 in the outlet gas stream also increased with the increase of water to ethanol ratio, while the formation of the byproducts, CO and methane, decreased with the increase of steam-to-ethanol molar ratio. Obviously, in accordance with the mass action law, at higher water to ethanol ratios, not only were the reforming reaction ,Reaction (2.5), and the shift reaction, Reaction (2.2), favored but also the reverse shift reaction, Reaction (2.10), could be inhibited. Similar observations were also reported for other catalyst systems. On the other hand, it would also be beneficial for the suppression of carbon deposit on the catalyst to conduct steam reforming of ethanol at a molar ratio of higher than the stoichiometric ones (Yang *et al.*, 2006).

2.2.2. Glycerol Steam Reforming

Glycerol is used in many applications including personal care, food, oral care, tobacco, polymer and pharmaceutical applications. However, significant growth of biodiesel industry has created the glycerol as feedstock having a demanded market value. Therefore using glycerol as a source of producing hydrogen became important (Adhikari *et al.*, 2007). In order to identify the effect of the aforementioned variables, thermodynamic analyses are employed for the steam reforming reaction of glycerol, Reaction (2.11), to maximize hydrogen yield and minimize undesirable products (Adhikari *et al.*, 2007).

$$C_3H_8O_3 + 3H_2O = 3CO_2 + 7H_2 \qquad \Delta H^0_{298} = 129.7 \text{ kJ/gmol} \quad (2.11)$$

Lou and coworkers (2007) have completed the thermodynamic analysis of three pyrolysis products; sorbitol, glycerol and ethylene glycol. They adopted MATLAB language to carry out the calculations assuming ideal state and real state using Peng - Robinson equation of state. Stoichiometric approach has been applied and besides the reforming reaction, Reaction (2.11), water gas shift and methanation (Reactions (2.2) and (2.7)), respectively have been taken into consideration. The investigated parameters were temperature (between 300 and 500 K) and pressure (between 1 to 50 atm) The fuels are assumed as liquid, water in both phases and other compounds CO, CO_2, H_2, and CH_4 are in gas phases (Luo *et al.*, 2007).

Reforming of bio oil products is different from the reforming of fossil fuels in the sense that the former can run at low reforming temperatures. When temperature is increased, the reforming equilibrium constant and, consequently, glycerol conversion is improved. The maximum hydrogen mole fraction in dry basis in glycerol reforming reaches to 70 per cent in the products. In addition reverse water gas shift reaction is promoted and more heat is given out from the methanation reaction leaving more CO in the system (Luo *et al.*, 2007).

Another analysis on the steam reforming process of glycerol is performed at pressure, temperature and steam-to-fuel ratio ranges of 1–5 atm, 600–1000 K, and 1–9, respectively by Adhikari and coworkers (2007). The results show that the number of moles of hydrogen increases with increasing temperature and steam-to-fuel ratio and with decreasing pressure. The effect of the pressure on the glycerol steam reforming process is found to be consistent with methanol and ethanol steam reforming processes. The mole fraction of hydrogen is found to be higher in case of low steam-to-fuel ratio. This is mainly due to the significant amount of water present in the product at high steam-to-fuel ratio (Adhikari *et al.*, 2007). Unreacted water reduces the mole fraction of hydrogen but not necessarily the quantity. The greatest quantity of hydrogen is produced at excess water at all temperatures. The best conditions to produce hydrogen will be with excess water if the purification problems can be overcome. The maximum hydrogen mole value per glycerol steam reforming is obtained as 6, at steam-to-fuel ratio is 9 under 960 K and P=1 atm while stoichiometric value is 7 (Adhikari *et al.*, 2007).

CH_4 production decreases when the temperature and the steam-to-fuel ratio increase. However, higher pressure favors the formation of CH_4. At higher S/F ratios, i.e., 9:1 and 6:1, and at higher temperatures (>950K), the formation CH_4 is almost inhibited. As the temperature increases, moles of water and CH_4 decrease with increasing CO, CO_2, and H_2. This can be attributed to the methane steam reaction to produce CO or CO_2 and H_2 (Adhikari *et al*, 2007). Number of moles of CO increases with the increase in temperature but decreases with increasing S/F ratio. However, the number of moles of CO_2 increases with increasing temperature, goes through maximum at around 850 K, and then decreases at higher temperatures. This behavior may be attributed to the reformation of CH_4 with CO_2. Carbon formation has also been investigated and it has been observed that at 1000 K

no carbon is formed at any S/F ratio. At S/F ratios of 6 and 9, carbon formation was thermodynamically inhibited at any temperature analyzed in this study. It has also been observed that carbon formation dropped significantly while S/F is increased from 1 to 3 (Adhikari *et al.*, 2007).

2.2.3. Ethylene Glycol Steam Reforming

Ethylene glycol is one of the components of aqueous phase of bio oils and its concentration can reach up to 2 per cent. The hydrogen content in ethylene glycol reforming, Reaction (2.12), is similar to glycerol, resulting with a maximum of ca. 71.4 per cent by mole (dry basis) of hydrogen in the product mixture (Luo *et al.*, 2007). Besides the steam reforming, direct decomposition reactions increases the hydrogen production (Kechagiopoulos *et al.*, 2007).

$$C_2H_6O_2 + 2H_2O = 2CO_2 + 5H_2 \qquad \Delta H^0_{298} = 88.9 \text{ kJ/gmol} \quad (2.12)$$

Kechagiopoulos and coworkers (2007) have shown that steam reforming of ethylene glycol can give hydrogen yields up to 90% at reaction temperatures higher than 600°C and at S/C ratios higher than 3 with complete conversion of the organics. The results also indicate that hydrogen is produced not only by the steam reforming reaction but also by the decomposition of ethylene glycol. The main gaseous products are CO, CO_2, CH_4, H_2, C_2H_6 with smaller amounts of C_2H_4. CO and CH_4 appear due to side reactions of WGS and methanation leading to lower hydrogen content with respect to the maximum stoichiometric value. The effect of temperature on gas product composition is not particularly strong: at 650°C, 10 per cent of the converted ethylene glycol resulted in CH_4 with this value dropping below 5 per cent at 850°C. Part of ethylene glycol decomposes thermally, while the rest is reformed with steam towards H_2 and CO_x. The results obtained are not enough to claim about the parallel and/or consecutive reaction network of reforming and decomposition reactions.

Apart from the experimental studies, thermodynamic analyses are conducted under various conditions, at temperatures between 400 and 1300 K and at steam-to-fuel ratios between 1 and 9. The effect of pressure variation from 1 to 20 atm on the product

distribution is also investigated (Vagia and Lemonidou, 2007). Temperature effect is investigated at constant S/F ratio of 6. At low temperature (400 K), CH_4 and CO_2 are the only gaseous products formed via decomposition of the alcohol. On the other hand, high temperatures favor the production of hydrogen and carbon monoxide, while methane and carbon dioxide mole fraction decrease. Hydrogen mole fraction is found to approach 0.68 at 900 K while a slight decrease of its concentration is observed at higher temperatures (Vagia and Lemonidou, 2007).

Steam to fuel ratio has a strong influence on the reforming product distribution. Increasing S/F ratio favors the production of hydrogen and, as a result, maximum mole fraction of hydrogen approaches 0.69 at 900 K for the highest S/F value of 9. The higher the steam-to-fuel ratio, the lower the content of methane and carbon monoxide in the product mixture is observed. However, such a trend is not reported for CO_2 when temperature is lower than 800 K, the CO_2 content is almost independent of S/F, while at higher temperatures it is strongly related to steam-to-fuel ratio. Steam-to-fuel ratio also affects carbon formation: ratios higher than 3 are reported to ensure carbon free operation (Vagia and Lemonidou, 2007).

Pressure has also an important effect on the product distribution, especially in the temperature range between 600 and 1000 K. Hydrogen and methane are the two products mostly affected by the pressure. Increase in the pressure from 1 to 20 atm results in a decrease of hydrogen molar fraction at 900 K from 0.68 to 0.49. Under same conditions methane content increases from 0 to 0.2. The direct relation between hydrogen and methane demonstrates that steam reforming of methane is the main route of hydrogen production. At temperatures higher than 1100 K the effect of pressure is negligible, since at this level the distribution of the products is mainly determined by water gas shift equilibrium, a reaction with no volume variation. Increased pressure does not favor carbon formation, which remains negligible under all conditions examined S/F = 6 and temperature 400–1300 K. The results reveal that pressure is one of the critical factors, which affect the equilibrium state demonstrating that it is desirable to keep the pressure of the reactor as low as possible in order to maximize hydrogen production. However, to maintain a high degree of hydrogen production efficiency, in case that higher pressure is

necessary for the target process of hydrogen utilization, reaction temperatures higher than 1100 K should be applied (Vagia and Lemonidou, 2007).

2.2.4. Acetic Acid Steam Reforming

Acetic acid comes from the acetyl groups of hemicelluloses and has been identified as one of the major organic acids and components (up to 12 per cent by volume) present in the aqueous phase of bio oil (Bimbela *et al.*, 2000; Yaman, 2004). Therefore steam reforming of this model compound has also been studied (Basagiannis and Verykios, 2007):

$$C_2H_4O_2 + 2H_2O = 2CO_2 + 4H_2 \qquad \Delta H^0_{298} = 134.6 \text{ kJ/gmol} \quad (2.13)$$

The equilibrium mixture formed by reforming of acetic acid consists of hydrogen, carbon monoxide and dioxide, methane, unconverted steam and coke (carbon). Hydrogen yield is always under the stoichiometric maximum value due to undesirable side reactions such as WGS and methanation giving out more CO and CH_4 as side products (Bimbela *et al.*, 2000).

The results obtained by Vagia and Lemonidou (2007) show that at temperatures higher than 900 K hydrogen content is a weak function of temperature: its mole fraction decreases from 0.63 to 0.60 when the temperature is increased from 900 to 1300 K. The decrease in hydrogen content is accompanied by an increase in carbon monoxide, which is primarily due to water gas shift reaction equilibrium. As the temperature increases, hydrogen appears as a product at the expense of methane. The methane mole fraction decreases to zero at 900 K, a temperature at which hydrogen mole fraction attains maximum at S/F of 9, demonstrating that H_2 formation route parallels with CH_4 consumption (Vagia and Lemonidou, 2007).

It has been reported that steam-to-fuel ratio affects both the methane and carbon monoxide concentrations (Adhikari *et al.*, 2007). The former is found to decrease with increasing steam-to-fuel ratios. Production of carbon monoxide is negligible up to 600 K, while the effect of steam-to-fuel ratio becomes important at temperatures higher than 700

K. Higher concentrations of water in the feed mixture disfavor the formation of CO over the whole range of (Adhikari *et al.*, 2007).

A variety of catalysts are also tested under conditions of steam reforming of acetic acid by Basagiannis and Verykios (2007). It is observed that, CO and CO_2 are the only products other than hydrogen, implying that the reaction of steam reforming of acetic acid along with the WGS reaction are the two reactions which take place within investigated temperature range. However, at temperatures lower than 650°C hydrogen selectivity is reduced due to the formation of by-products, such as acetone and trace amounts of methane. Observed products, H_2, CO and CO_2, are very close to those defined by thermodynamic equilibrium under the present conditions (Basagiannis and Verykios, 2007).

In another experimental study, acetic acid solutions corresponding to a specific steam-to carbon molar ratio are used to confirm the theoretical results (Bimbela *et al.*, 2000). In this study, steam-to carbon ratio is kept constant at 5.58, temperature was set to 550, 650 and 750°C, and product distribution at steady state is investigated. The results show that the molar distribution of hydrogen, carbon monoxide and carbon dioxide was 65, 5 and 30 per cent, respectively. As the temperature is increased compositions of carbon monoxide and carbon dioxide changed, whereas composition of hydrogen remained almost unchanged: molar gas composition (N_2 and H_2O free basis) is again around 65 per cent for hydrogen but CO and CO_2 gas yields vary significantly with temperature, increasing from around 4 per cent at 550°C up to around 8 per cent for CO, whereas CO_2 decreases from around 30 per cent down to 26 per cent (Bimbela *et al.*, 2000).

2.2.5. Acetone Steam Reforming

Acetone, C_3H_6O, is the model compound selected as a representative of the ketones present in bio-oil at appreciable amounts up to 2.8 per cent. Steam reforming of acetone can be described by the following reaction:

$$C_2H_6O + 5H_2O = 3CO_2 + 8H_2 \qquad \Delta H^0_{298} = 245.0 \text{ kJ/gmol} \quad (2.14)$$

Equilibrium calculations were performed under the same operating conditions as for the acetic acid (Basagiannis and Verykios, 2007). Full conversion of oxygenate is attained even at the lowest temperature examined. The mole fraction of the products formed from acetone steam reforming as a function of temperature from 400 to 1300 K show that the maximum hydrogen content 0.68–0.69 is attained at 900–1000 K while further increase of temperature slightly decreases its concentration to the equilibrium mixture. In general, hydrogen mole fraction is found to increase with steam-to-fuel ratio. High steam to fuel ratio and temperature result in the consumption of methane, which is completed at temperatures higher than 1000 K. At the steam-to-fuel ratio of 9, methane prevails over CO_2 at low temperature while gradual increase of temperature is accompanied by the rise in hydrogen content and the respective decline in methane. Carbon monoxide emerges as a product at higher than 700 K and its concentration monotonously increases up to 0.2 at 1300 K. Lowest carbon monoxide concentration is attained at the highest steam-to-fuel ratio used (Vagia and Lemonidou, 2007).

Carbon dioxide concentration is a strong function of steam-to-fuel ratio and the temperature. Its content passes through a maximum at relatively low temperatures for steam-to-fuel less than 6 drifting to lower values at higher temperature levels (Resini *et al.*, 2005). Carbon selectivity results of acetone reforming show that at temperatures lower than 900 K is more than 50 per cent of the carbon atoms of acetone are converted to carbon. Even at 1300 K, one over three-carbon atoms is not converted to gaseous reforming products. The threshold for carbon free operation is found as steam-to-fuel of 3 at temperatures higher than 1000 K, whereas the steam-to-fuel ratio limit increases to 6 when the temperature is reduced to 500 K (Vagia and Lemonidou, 2007).

2.2.6. Phenol Steam Reforming

Phenol is one of the components that appear in the bio-oil mixture at compositions around 2-6 per cent (Iojoiu *et al.*, 2007), but the information available for its steam reforming is scarce:

$$C_6H_6O + 11H_2O = 6CO_2 + 14H_2 \qquad \Delta H^0_{298} = 395.4 \text{ kJ/gmol} \quad (2.15)$$

$$C_6H_6O + 5H_2O = 6CO + 8H_2 \qquad \Delta H^0_{298} = 642.3 \text{ kJ/gmol} \quad (2.16)$$

Polychronopoulou and coworkers (2004) have studied phenol steam reforming at a temperature range of 575–730°C over commercial Ni-based catalyst. They found that the H_2 concentration increases with increasing concentration of H_2O in the feed stream at all reaction temperatures studied. In particular, at 575°C the hydrogen concentration is found to increase approximately by 70 per cent by increasing the H_2O concentration in the feed from 20 to 40 per cent The phenol conversion was found to be 20.3 and 45.0, while the hydrogen selectivity, was 38.0 and 51.6 per cent in the case of using 20 and 40 mol per cent H_2O in the feed stream, respectively. This result supports the hypothesis that the reaction order with respect to H_2O is positive for the water–gas shift reaction towards CO_2 and H_2 formation in the 575–730°C range. It is pointed out again the positive order of reaction with respect to water concentration since the conversion of phenol increases with increasing water feed concentration at all reaction temperatures studied (Polychronopoulou *et al.*, 2004)

2.2.7. 2-propanol Steam Reforming

2-propanol or isopropyl alcohol (IPA) is also used as a washing agent and large amounts of it are given out as waste solution. This solution is then utilized for thermal energy production in boilers but there are alternative routes to qualify this compound such as steam reforming with an efficient catalyst for hydrogen production. Studies related to steam reforming of IPA is scarce, but existing studies indicate that at temperatures lower than 673 K, IPA was hardly steam reformed but converted to propene and/or acetone, while at a higher reaction temperatures CO, CH_4, CO_2, C_3H_6 appeared as products with different distributions ratios (Mizuno *et al.*, 2003)

2.3. Deterministic Optimization Techniques

Optimization aims to find the optimum solution of a specific problem. The system under investigation is described with an objective function including variables, which represents the unknown characteristic of the system. During process the optimum solution

is searched according to some limitations named as constraints (Nocedal and Wright, 1999).

Optimization algorithms are not unique and there are numerous routes feasible for a particular problem. The choice of algorithms depends upon the requirement of the solution accuracy or speed of the optimization (Nocedal and Wright, 1999). Mainly, optimization methods are classified in two groups; deterministic methods and stochastic/probabilistic methods depend upon the solution pathway (Floudas, 1997).

Deterministic methods use objective function and gradient information to reach the optimization whose solutions depend upon the initial guess. In this method, objective function and constraints must be continuously differentiable. For smooth function which shows the convex property, every minimum is the local minimum for which deterministic algorithms are very powerful with its quick solution routes (Lasdon, 2001). One main failure of the deterministic algorithms is that they calculate point by point starting from initial conditions and global optimum may not be reached if the iteration is trapped in the local one which may be very far away the real global optimum (Floudas, 1997)

Deterministic methods are applied in many chemical engineering problems, such as control parameters, kinetic parameter estimations, phase and chemical equilibrium determination in which the objective function can be non-linear and multivariable leading to nonconvex property having several local optimums in which global optimization becomes important. In global optimization aim is to compute and identify the global optima, either minimum or maximum, of the functions generally nonconvex in nature, under the predetermined variable limits (Floudas *et al.*, 2005). However, these currently available methods are generally very expensive (Nichita *et al*., 2002).

Many studies are performed for estimating equilibrium compositions in chemical and phase equilibrium problems, whose natures are generally non-convex and their solution depend on the given set of initial guess. Therefore, several papers have been published focusing on accurately determining the equilibrium composition and ensuring convergence of chemical and phase equilibrium problems via minimization of Gibbs free energy. The ways are Interval Newton method, branch and bound framework (Esposito *et al*, 2000),

nonlinear programming methods (NLP), mixed-integer nonlinear optimization (MINLP), successive quadratic programming (SQP) and successive linear programming (SLP) (Lasdon, 2001). Lipschitz algorithm, Homotopy continuation method, SLP and SQP can be explained as the improved version of algorithms to the solution of highly nonlinear problem.

SQP methods are appropriate for solving optimization problems with sufficiently high precision provided that the level of nonlinearity of the objective function and the number of parameters are low. The solution procedure is based on formulating and solving a quadratic sub-problem in each iteration. The sub-problem is obtained by linearizing the constraints and by approximating the Lagrangian function quadratically (Mansoornejad, 2008).

3. MATHEMATICAL TECHNIQUES FOR THE PREDICTION OF CHEMICAL REACTION EQUILIBRIUM

The present work involves the thermodynamic analysis of steam-driven conversions of a set of oxygenated hydrocarbons, namely formic acid, lactic acid, isopropyl alcohol and phenol, which are components of bio-oil. The analysis is done at a temperature interval of 600-1000 K at which the hydrocarbons are in their vapor phase, and, therefore, the presence of gaseous species are considered. The equations given in this chapter are formulated based on the presence of a single (vapor) phase.

3.1. Introduction to Mathematical Techniques for Chemical Equilibrium

Thermodynamic analysis is the determination of the equilibrium state of the chemical processes for both reacting and non-reacting systems. The phase and the component distribution of a particular system are determined with respect to the specified operating parameters (Floudas, 2000). There are two general approaches to equilibrium modeling: stoichiometric and non-stoichiometric (Adhikari *et al*., 2007).

First modeling approach is based on the equilibrium constants of the predetermined reaction in which the stoichiometric relation of the possible reactions should be clearly defined (Adhikari *et al*., 2007). This one is favored when the reaction kinetics and mechanism are well known but the major failure of this method is that if a wrong reaction is considered or if there is a missing reaction expression, the results may change significantly (Mas *et al*., 2006).

Second modeling approach involves the use of Gibbs free energy minimization method, including the determination of equilibrium composition of the possible products by making the total Gibbs free energy of the system at its minimum in accordance with constraints generated by the conservation of mass (Adhikari *et al*., 2007). The basis of this method comes from the fact that the system is thermodynamically favored when its Gibbs Free Energy (GFE), expressed as a function of pressure P, temperature T, and the concentration of the different components (Sandler, 1998), is at its minimum value (McDonald and Floudas, 1994). Main benefit of this method is that it does not require the

knowledge of the chemical reactions that take place at equilibrium. This method is particularly suitable for unclear reaction mechanisms and feed streams like biomass whose precise chemical compositions of the products are not known.

Up to now many optimization techniques are employed to determine the minimum value of the Gibbs free energy function such as Lagrange multipliers (Lwin *et al*., 2000) or direct minimization methods using traditional mathematical tools for a single phase or multiphase calculations of the minimum GFE (Faungnawakij *et al*., 2006). Recently, commercial simulation suites such as, Aspen plus (Wang *et al*., 1997), (Vagia and Lemonidou, 2007), (Seo *et al*., 2002), Aspen Tech™ (Semelsberger and Borup, 2005) or Chemkin (Lutz *et al*., 2003) are applied which interface the similar or up to date deterministic optimization algorithms.

In this work, thermodynamic analyses of the vapor-phase steam driven conversions of four selected bio oil hydrocarbons – formic acid, isopropyl alcohol, lactic acid and phenol – are performed by minimization of the total Gibbs free energy and the effects of temperature, pressure and inlet steam-to-fuel ratio on the equilibrium product distribution are investigated. The resulting objective function is optimized using deterministic approach and results are presented in Chapter 4 by using the Sequential Quadratic Programming optimization technique.

3.2. Mathematical Formulation of the Gibbs Free Energy Minimization

Total Gibbs free energy function represents the sum of Gibbs free energy of all components at equilibrium state and obtained by multiplying the molar Gibbs free energy of the component with its molar value in the system (Faungnawakij *et al*., 2006; Lwin *et al*., 2000). G^t is defined as the total Gibbs free energy,

$$G_t = \sum_{i \subset C} n_i \cdot \bar{G}_i \tag{3.1}$$

The molar Gibbs free energy function is the chemical potential of the component in isobaric and isothermal conditions, $\overline{G_i}$, which is derived from the addition of formation of

Gibbs free energy at ideal states to differentiation relations from ideal states (Faungnawakij *et al*., 2006):

$$\overline{G}_i = G^0_{i,f} + R \cdot T \cdot ln(\frac{\hat{f}_i}{f^0_i}) \tag{3.2}$$

There are two important observations in regard of the optimization formulation; in ideal conditions, the constraint set is of small size and linear, but nonlinearity appears in the objective function (Floudas, 2000). The main difficulty is due to the complex nature of the models used to predict fugacities, which leads to highly nonconvex functionalities results. This may lead to local or trivial solutions that are not true equilibrium solutions, and may be far away from the correct optimum solution. In this case, the solution will also be very dependent on the chosen starting point (McDonald and Floudas, 1994).

3.2.1. Mathematical Formulation for Ideal Gas Model

If the system is ideal, then any local solution will be the global solution (McDonald and Floudas, 1994). Many algorithms have been used to minimize the total Gibbs free energy function under the assumption that if the system is ideal. The difference from the ideal gas assumptions is considered in the fugacity calculation of each pure component and fugacity of the mixture which is derived from the pure component values.

$$\frac{\hat{f}_i}{f^0_i} = \hat{\phi} \cdot x_i \cdot P \tag{3.3}$$

In Equation (3.3.) x_i is the mole fraction of the component and P is the system pressure. When the problem is solved under the ideal gas assumption, $\hat{\phi}$ is taken as unity, 1, and the Equation (3.3) is simplified and inserted to Equation (3.2) and finally Equation.(3.4) is obtained as the objective function.

$$\overline{G}_i = G^0_{i,f} + R \cdot T \cdot ln(x_i \cdot P) \tag{3.4}$$

Even if Equation (3.4) is nonlinear, most of the optimization algorithms are powerful to handle this minimization with the elemental constraints mentioned in Section 3.2.3

Table 3.1. Equations of the Ideal Modeled Optimization (Sandler, 1989; Floudas, 2000)

Function	Expression
Objective Function	$G_t = \sum_{i \subset C} n_i \cdot (G^0_{i,f} + R \cdot T \cdot ln(\frac{n_i}{n_t} \cdot P))$ (3.4)
Linear Constraints	$n_t - \sum_{i \subset C} n_i = 0$ (3.5)
	$\sum_{k \subset e} a_{ei} \cdot n_i - b_e = 0$ (3.6)
Boundaries	$0 \le n_i \le n_t$ (3.7)

3.2.2. Mathematical Formulation for Non Ideal Gas Model

In contrast with the ideal case, the objective function is derived with the integration of equation of state into the problem for modeling the non-ideal case. From this addition, the nonlinearity of the total Gibbs free energy function increases and in optimization, finding the global minimum, which is defined as the true equilibrium state, becomes difficult to determine. Determination of this global minimum in some cases is difficult due to the non- convex property of the objective function when the system considered involving more than one phase. Note that, for the ideal cases, the objective function is simple and easy to solve, compared to non-ideal cases in which fugacity approach should be included into the calculations.

Fugacity coefficient depends upon the temperature, pressure and the component distribution of the system and should be determined for each condition of the system (Walas, c1985). Therefore the $\hat{\phi}$ term in Equation (3.3) should be calculated for each condition and inserted into the objective function, Equation (3.2).

Different equation of states (EOS) can be applied to calculate the fugacity coefficients. The frequently used EOS in the thermodynamic calculations are Soave-Redling-Kwong (SRK) (Harding and Floudas, 2000; Rangaiah, 2001) and Peng–Robinson (PR) (Luo *et al.*, 2007). The first one, SRK is a three-parameter equation of state and is quite convenient for users having a good trade-off between precision and complexity of the calculation (Walas, c1985). It is also widely applied in petrochemical processing computations. The polynomial form of the Soave-modified Redlich-Kwong equation of state for mixtures is in Equation (3.8);

$$z^3 - z^2 + (A^{mix} - B^{mix} - (B^{mix})^2) \cdot z - A^{mix} \cdot B^{mix} = 0 \tag{3.8}$$

The pressure-explicit form in Equation (3.9) can be expressed as follows:

$$P = \frac{R \cdot T}{V - B^{mix}} - \frac{A^{mix}}{V \cdot (V + B^{mix})} \tag{3.9}$$

The pure component parameters needed to evaluate the mixture values are given as follows:

$$m_i = 0.48 + 1.574 \cdot w_i - 0.176 \cdot w_i^2 \tag{3.10}$$

$$A_i = 0.42747 \cdot \frac{P \cdot T_{c,i}^2}{P_{c,i} \cdot T^2} \cdot \left[1 + m_i \cdot (1 - \sqrt{\frac{T}{T_{c,i}}}) \right]^2 \tag{3.11}$$

$$B_i = 0.08664 \cdot \frac{P \cdot T_{c,i}}{P_{c,i} \cdot T} \tag{3.12}$$

From these pure component properties the following relations are employed to establish the mixture properties:

$$A^{mix} = \sum_{i \subset C} \sum_{j \subset C} x_i \cdot x_j \cdot A_{i,j} \tag{3.13}$$

$$B^{mix} = \sum_{i \subset C} x_i \cdot B_i \tag{3.14}$$

$$A_{i,j} = (1 - k_{i,j}) \cdot \sqrt{A_i \cdot A_j} \tag{3.15}$$

When these expressions are inserted into Equation (3.16), the fugacity coefficient of a component in a mixture can be obtained as follows for each condition depending on the change in temperature, pressure and mole fractions:

$$ln(\hat{\phi}_i) = \frac{B_i}{B^{mix}} \cdot (z-1) - ln(z - B^{mix}) + \frac{A^{mix}}{B^{mix}} \cdot \left[\frac{B_i}{B^{mix}} - \frac{2}{A^{mix}} \cdot \sum_{j \subset C} x_j \cdot A_{ij} \right] \cdot ln\left(1 + \frac{B^{mix}}{z}\right) \tag{3.16}$$

Addition of this term into total Gibbs free energy equation makes the form highly nonlinear and non-convex Equation (3.17) in which simple optimization routes may fail to solve.

Table 3.2. Equations of the Non Ideal Modeled Optimization (Harding and Floudas, 2000)

Function	Expression
Objective Function	$G_{total} = \sum_{i \subset C} n_i \cdot G^0_{i,f} + \sum_{i \subset C} n_i \cdot R \cdot T \cdot \left(\begin{array}{l} ln\left(\frac{n_i}{n_j}\right) + ln(P) + \frac{B_i}{B^{mix}} \cdot (z-1) - ln(\omega) \\ + \frac{A^{mix}}{B^{mix}} \cdot \left(\frac{B_i}{B^{mix}} - \frac{2}{A^{mix}} \cdot \alpha_i \cdot ln\left(1 + \frac{B^{mix}}{z}\right) \right) \end{array} \right)$ (3.17)
Nonlinear Constraints	$z^3 - z^2 + (A^{mix} - B^{mix} - (B^{mix})^2) \cdot z - A^{mix} \cdot B^{mix} \le 0$ (3.8)
	$z^3 - z^2 + (A^{mix} - B^{mix} - (B^{mix})^2) \cdot z - A^{mix} \cdot B^{mix} \ge 0$ (3.8)
	$A^{mix} - \sum_{i \subset C} \frac{n_i}{n_t} \cdot \alpha_i = 0$ (3.18)
	$\alpha_i - \sum_{j \subset C} \frac{n_j}{n_t} A_{ij} = 0$ (3.19)
	$B^{mix} - \sum_{i \subset C} \frac{n_i}{n_t} \cdot B_i = 0$ (3.14)

Table 3.2. (continued) Equations of the Non Ideal Modeled Optimization (Harding and Floudas, 2000)

Function	Expression	
Linear Constraints	$n_t - \sum_{i \subset C} n_i = 0$	(3.5)
	$\sum_{k \subset e} a_{ei} \cdot n_i - b_e = 0$	(3.6)
	$-\omega + z - B^{mix} = 0$	(3.20)
Boundaries	$0 \le n_i \le n_t$	(3.7)
	$z > 0$	(3.21)
	$\omega > 0$	(3.22)

3.2.3. Elemental and Feasibility Constraints

There are some mathematical constraints that dictate the physical and chemical limitations of a reacting system. In other words, the minimization of Equation (3.2) should satisfy the conservation of mass, so some additional constraints are required for obtaining feasible solutions that are physically consistent. These are called elemental constraints and mass balance constraints. In view of the mass balance, the number of moles of any element in the product stream must equal to that existing in the feed stream. For the conservation of the number of atoms in the system Equation (3.14) is employed.

$$\sum_{k \subset e} a_{ei} \cdot n_i - b_e = 0 \tag{3.6}$$

In Equation (3.14) a_{ei} represents the number of gram atoms of element e existing in the component i, and b_e is the total number of element e in the system (Floudas, 2000). During equations the mole fractions of the compounds are required so these values are obtained division of moles of a component to the sum of moles. During iterations this value, n_t, should also be satisfied with the linear constraint given in Equation (3.15)

$$n_t - \sum_{i \subset C} n_i = 0 \tag{3.5}$$

For the feasibility of the solutions, each mole value on the iteration must be positive, having some physical meaning and should be lower than the total number of moles in the system (Floudas, 2000):

$$0 \leq n_i \leq n_t \tag{3.7}$$

When the equations are inserted into the optimization algorithm, some additional variables and boundaries are required. Variables a_i and w are added into the calculations to lower the non-linearity, to simplify the solution of fugacity constraints and to prevent the division by zero during calculations.

3.3. Optimization via Sequential Quadratic Programming

Two models, ideal (Section 3.2.1) and non-ideal (Section 3.2.2), were solved using GAMS which interface different nonlinear solvers. SNOPT (Sparse Nonlinear Optimizer) is chosen as the required solver option which implements a sequential quadratic programming (SQP) method for solving constrained optimization problems with smooth nonlinear functions in the objective and constraints. Figure 3.1 gives the general optimization problem which can be solved by SNOPT (Gill et al., 2002).

minimize or	maximize $f(x)$
	$F(x) \sim b_1$
subject to	$G(x) \sim b_2$
	$l \leq x \leq u$

Figure 3.1. General Optimization Problem for SNOPT algorithm

In Figure 3.1, $f(x)$ is a linear or nonlinear smooth objective function, l and u are constant lower and upper bounds, $F(x)$ is a set of nonlinear constraint functions, $G(x)$ is a sparse matrix, ~ is a vector of relational operators ($\leq$, $\geq$ or =), and b_1 and b_2 are right-hand

side constants. $F(x) \sim b_1$ are the nonlinear constraints of the model and $G(x) \sim b_2$ forms the linear constraints. The gradients of f and F_i are automatically provided by GAMS, using its automatic differentiation engine (Gill *et al.*, 2002).

The nonlinear objective functions having linear constraints as in the ideal gas problem can be solved easier than the one having nonlinear constraints. (i.e. Equations (3.10), (3.11) or (3.12)) GAMS works with an objective variable which represents the objective function but in SNOPT this variable is converted to an objective function and problem is solved with application of a sparse sequential quadratic programming (SQP) implemented into SNOPT (Gill *et al.*, 2002).

Sequential quadratic programming (SQP). is an optimization algorithm for nonlinear optimization problems when the problem is smooth, not large and gradients can be evaluated with high precision. All the functions (i.e. Figure 3.1), including the objective function $f(x)$ and constraints $G(x)$ must be continuously differentiable (Mansoornejad *et al.*, 2008). The essential idea in the SQP is to model a quadratic sub-problem at the current x_k, and minimizing this new subproblem in which new iterate x_{k+1} could be obtained with good convergence and good performance of the overall algorithm (Nocedal and Wright, c1999).

The sub-problem is obtained by linearizing the constraints and approximating the Lagrangian function quadratically as in Equation (3.23)

$$L(x, \lambda) = f(x) - \lambda^T \cdot G(x) \tag{3.23}$$

At each iteration, an approximation is made of the Hessian of the Lagrangian function using a Quasi-Newton updating method. The process would be proceeded from given iteration x_k, which is an approximation of the solution, λ_k an approximation of the multiplier and H_k which is an approximation of the Hessian of the Lagrangian function. Then, the following quadratic programming (QP) sub-problem is formed to solve:

$$\text{minimize} \quad d^T \cdot H_k \cdot d + \nabla f(x_k)^T \cdot d \tag{3.24}$$

$$\text{subject to,} \quad \nabla G_i \cdot (x_k)^T \cdot d + G_i \cdot (x_k) = 0 \tag{3..25}$$

$$\nabla G_i \cdot (x_k)^T \cdot d + G_i \cdot (x_k) \geq 0 \tag{3.26}$$

The matrix H_k is a positive definite approximation of the Hessian matrix of the Lagrangian function. This sub-problem is a QP subproblem whose solution is used to form a search direction d_k for a line search procedure. In other words, the solution is used to form the next iterate: $x_{k+1} = x_k + \alpha_k . d_k$. The step length parameter α_k is determined by an appropriate line search procedure so that a sufficient decrease in a merit function is obtained (Mansoornejad et al., 2008).

3.4. Application of SQP to Solution of GFE Minimization Problems

During optimizations via GAMS, it is observed that for ideal gas modeling, evaluation of the optimum number of moles giving the lowest total Gibbs Free Energy value can be completed very quickly, i.e. the global optimum can be obtained. However, when the equation of state is used for handling calculations at high pressure, the problem becomes complex due to the presence of nonlinear constraints. In addition, the complexity of the solution increases further with the complexity of the fugacity coefficient determination in which the nonlinear constraints are involved solving the compressibility factor. This complexity also varies with the type of component, each having different thermodynamic constants and reaction stoichiometries. In such cases, it is observed that, the optimization problem either cannot be solved for all conditions of the range of thermodynamic analysis or, tough a solution is obtained, the results do not match with the physical phenomena.

This failure of the method emerges in many different values of the initial conditions and boundaries of the variables, all of which can be attributed to the general lack of the deterministic algorithms: the optimum solution may not be reached at all conditions in which the algorithm ends up with local points giving numerous results having no physical meaning in the solution. Therefore, in order to provide results close to the physically expected ones, some rearrangements are performed on the optimizations algorithm. An important parameter having significant effect on the solution is the compressibility factor, which exists in the model equation with the highest nonlinearity (Equation 3.16). In order

to observe the effect of bounding, the boundaries of the compressibility factor are narrowed down to 0.7–1 and 0.9-1 intervals.

Table 3.3. SQP results under different z boundaries (phenol steam reforming at 30 bar)

	S/F=4		S/F=5		S/F=7		S/F=9	
T (K)	0.7	0.9	0.7	0.9	0.7	0.9	0.7	0.9
600	+	+	+	+	+	+	+	+
700	+	+	+	+	+	+	+	+
800	-	+	-	+	-	+	+	+
1000	-	-	-	+	-	+	-	+

Table 4.6 indicates the convergence and failure points of the optimizations of steam reforming of phenol under different ranges of the compressibility factor, namely 0.7-1 and 0.9-1. The positive labels in Table 4.6 show that the convergence is obtained at the global level, whereas the negative labels indicate either a 'no-solution' case or the termination of the algorithm without global convergence. It can be observed that, as the z-interval is narrowed down, the number of globally converging solutions are increased. The results also show the dependence of the solution on the operating conditions, i.e. temperature and steam-to-fuel ratio, which is more notable at wider z-interval.

In order to implement further improvement, the expected product distribution is used during the solution. In other words, the results obtained from the ideal gas solutions are used as the reference results with +/- 20 per cent margin for the possible deviations at higher pressures. Therefore, in addition to the use of 'z-boundary', new boundaries for the number of moles of each species are inserted to the model for optimizations at 30 bar. The results showed that this implementation has led to the successful convergence at high-pressure cases regardless of the value of temperature and steam-to-fuel ratio. In other words, the negative labels given in Table 4.6 are turned into positive.

4. RESULTS AND DISCUSSION

Thermodynamic analyses of vapor phase steam reforming of four selected components of bio oil; formic acid, isopropyl alcohol, lactic acid and phenol are carried out using the Gibbs Free Energy Minimization technique. The resulting optimization problem is solved by employing the Sequential Quadratic Programming (SQP) optimization routine within the General Algebraic Modeling System (GAMS) environment. Two different approaches are employed for simulating different operating pressures, 1 bar and 30 bar. The gases are assumed to behave ideally in the former case and, therefore, fugacity coefficients are taken as unity and optimizations are performed. Simulation of the high-pressure case, on the other hand, involved the use of real (non-ideal) gas properties, during which the fugacity coefficients are derived from an equation of state (EOS) and implemented into the calculations. In order to determine the plausible products of the system a series of preliminary runs are conducted with isopropyl alcohol and phenol, the higher-carbon number components, by assuming product spectra including H_2, CO, CO_2 CH_4, C_2H_2, C_2H_4, C_2H_6, C_3H_4, C_3H_6, C_3H_8, C_5H_8, C_5H_{10}, C_5H_{12}. It was figured out that, the species that showed up in the product mixture were H_2, CO, CO_2 and CH_4. A similar trend is also reported in the theoretical and experimental studies involving steam reforming of C_2-C_4 oxygenated hydrocarbons (Faungnawakij *et al*., 2006). Therefore, H_2, CO, CO_2 and CH_4 are considered as the components of the product mixture and the analyses are conducted at temperature and steam-to-fuel ratio ranges of 600–1000 K and 4–9, respectively. The results are expressed in terms of mole fractions of the species which are calculated and plotted on dry-basis.

4.1. Results of Thermodynamic Analysis at 1 bar

In these sets of thermodynamic analyses calculations, all of the species are assumed to behave ideally, and, therefore, their fugacity coefficients are taken as unity. This approach allowed using the ideal-gas equation of state such that the presence of multimodal points in the objective function is eliminated. Therefore the optimum results, i.e. number of moles of each species at the minimum total Gibbs free energy of the system were obtained without any requirement of initial guess or predetermined boundaries.

During the simulation of each bio oil component, it is observed that the feed (i.e. formic acid, isopropyl alcohol, lactic acid, phenol), whose amount is considered as 1 mole, is converted almost completely to the products within the whole range of operating conditions (steam-to-fuel = 4-9; temperature = 600-1000 K; pressure = 1-30 bar). In other words, the product mixture is composed of hydrogen, carbon monoxide, carbon dioxide, methane and water (steam). However, the results, i.e. the mole fractions, are given on dry basis, i.e. the total number of moles is calculated by excluding water. This is due to the fact that most of the product mixture is composed of water, especially in cases where high steam-to-fuel ratios are selected. This eventually causes a sort of 'dilution' effect and prevents observing the trends of mole fractions of other species.

4.1.1. Formic Acid

The calculations are performed for hydrogen production from formic acid in the presence of steam. In such conditions, the formic acid does not give a reforming reaction but release its hydrogen content directly with a dehydrogenation reaction as given in Reaction (4.1):

$$CH_2O_2 = CO_2 + H_2 \qquad \Delta H^o_{298} = -14.91 \text{ kJ/mol} \quad (4.1)$$

Figure 4.1 gives equilibrium compositions of the species – hydrogen, carbon monoxide, carbon dioxide and methane – at the ranges of steam-to-fuel and temperature values investigated.

The results show that, the H_2 content is increased in the temperature range of 600 - 700 K whereas it remained almost constant between 700 -1000 K. This trend can be explained via the reverse water gas shift (RWGS), Reaction (2.10), and the methanation ,Reaction (2.7), reactions:

The enthalpy of reactions indicate that the methanation reaction is favored at lower temperatures more than dehydrogenation and RWGS due to its strong exothermicity. This will lead to the production of methane at lower temperatures (600 K). However the increase in temperature from 600 to 700 K will facilitate the conversion of methane to

hydrogen via reverse of reaction. This is believed to be the reason of the increase of hydrogen mole fraction between 600 – 700 K. At this temperature range amount of CO_2 decreases in accordance with the thermodynamics of endothermic RWGS and exothermic dehydrogenation reaction. The mole fraction of CO is 0.013 at 800 K but increases to 0.035 at 1000 K (Figure 4.1b). On the other hand, mole fractions of hydrogen and CO_2 decreases from 0.493 to 0.483 and from 0.494 to 0.483, respectively (Figures 4.1a and 4.1c). This behavior between 800 and 1000 K indicates the effect of the RWGS on the product distribution.

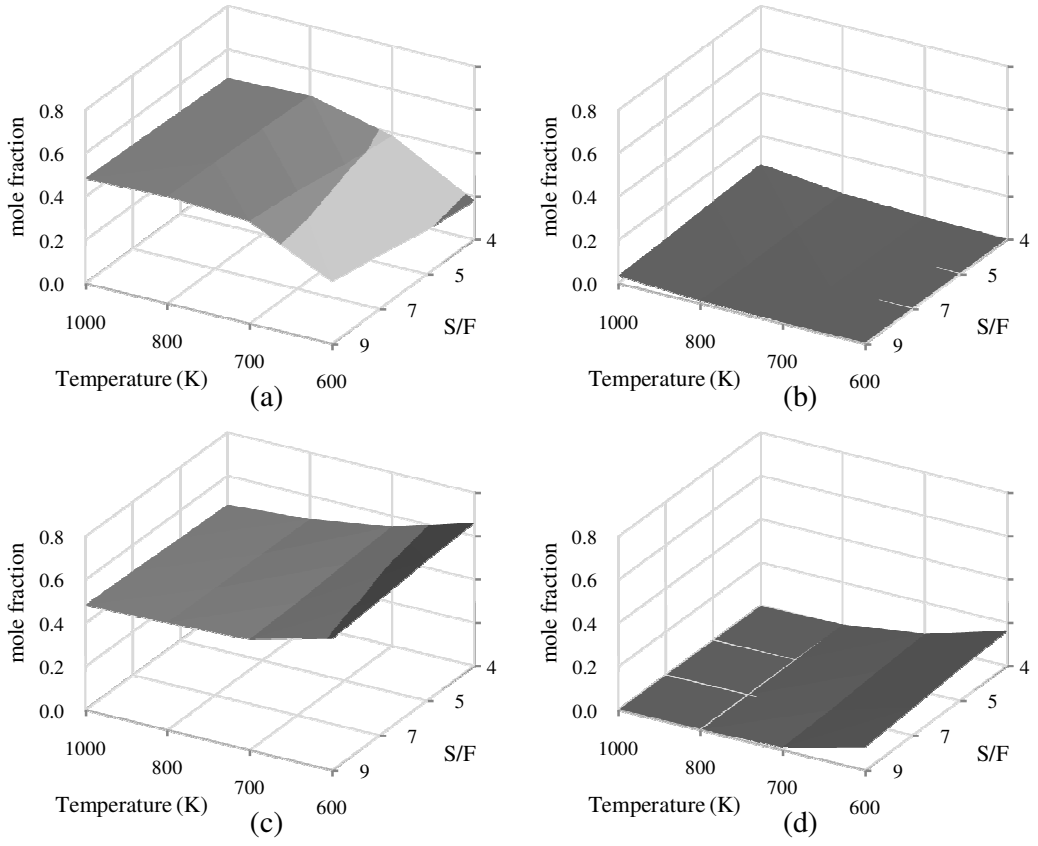

Figure 4.1. Effects of temperature and steam to fuel ratio on the mole fractions of the products during Formic Acid conversion (dry basis, 1 bar) (a) H_2, (b) CO, (c) CO_2, (d) CH_4

Steam to fuel ratio is found to affect the product distribution. For example, mole fraction of hydrogen is found to have increase 0.177 to 0.285 (61 per cent) at 600 K whereas the increase is only from 0.466 to 0.483 (3.6 per cent) at 1000 K. This is due to

the fact that, increase in the amount of steam shifts the equilibrium of methanation ,Reaction (2.7), in the direction of hydrogen formation; this can also be seen from the decreasing mole fraction of methane at high steam to fuel ratios (Figure 4.1d). At 1000 K, on the other hand, the increase in hydrogen seems to be due to the WGS (Figure 4.1a). This is supported by the slightly increasing trend of CO_2 from 0.466 to 0.483 (Figure 4.1c). and slightly decreasing trend of CO from 0.069 to 0.035 (Figure 4.1b). Note that, the change is limited since the temperature and steam to fuel have opposite effects on the WGS equilibrium.

4.1.2. Isopropyl Alcohol

The second fuel is the isopropyl alcohol which can be reformed as described in the reactions given below:

$$C_3H_8O + 5H_2O = 3CO_2 + 9H_2 \qquad \Delta H^o_{298} = 301.29 \text{ kJ/mol} \quad (4.2)$$

$$C_3H_8O + 2H_2O = 3CO + 6H_2 \qquad \Delta H^o_{298} = 424.74 \text{ kJ/mol} \quad (4.3)$$

Both of these reactions are endothermic and facilitated by temperature. This is best observed in Figure 4.2a which shows that increase in temperature leads to the rise in the mole fraction of hydrogen: its maximum value of 0.714 has been obtained at S/F=9 and at 1000 K (Figure 4.2a). Comparison of Figures 4.2b and 4.2c show that CO_2 production is already significant at 600K – the lower boundary of the temperature range – whereas evolution of CO becomes notable at temperatures higher than 700 K. Such an outcome is expected when the enthalpies of Reactions (4.2) and (4.3) are taken into account: the CO producing reaction needs higher temperatures to run and vice versa. There is, however, an interesting trend between CO_2 and hydrogen: although hydrogen and CO_2 are the products of the Reaction (4.2), the former increases with temperature, as stated above, whereas the latter exhibits a decreasing trend. This is most likely due to the RWGS, Reaction (2.10), which is endothermic, favored at high temperatures, and, therefore consumes CO_2 (Figure 4.2c). Hydrogen, the second reactant of RWGS, does not show the same decrease because endothermic methane steam reforming, Reaction (2.1), is likely to become significant at temperatures higher than 700 K, which can compensate the consumption of H_2. Note that,

methane steam reforming can yield 3 moles of hydrogen whereas RWGS can remove only one mole of hydrogen. The existence of RWGS and steam reforming can be further verified by the behavior of CO, which exhibits the highest rate of increase between 800-1000 K interval (Figure 4.2b).

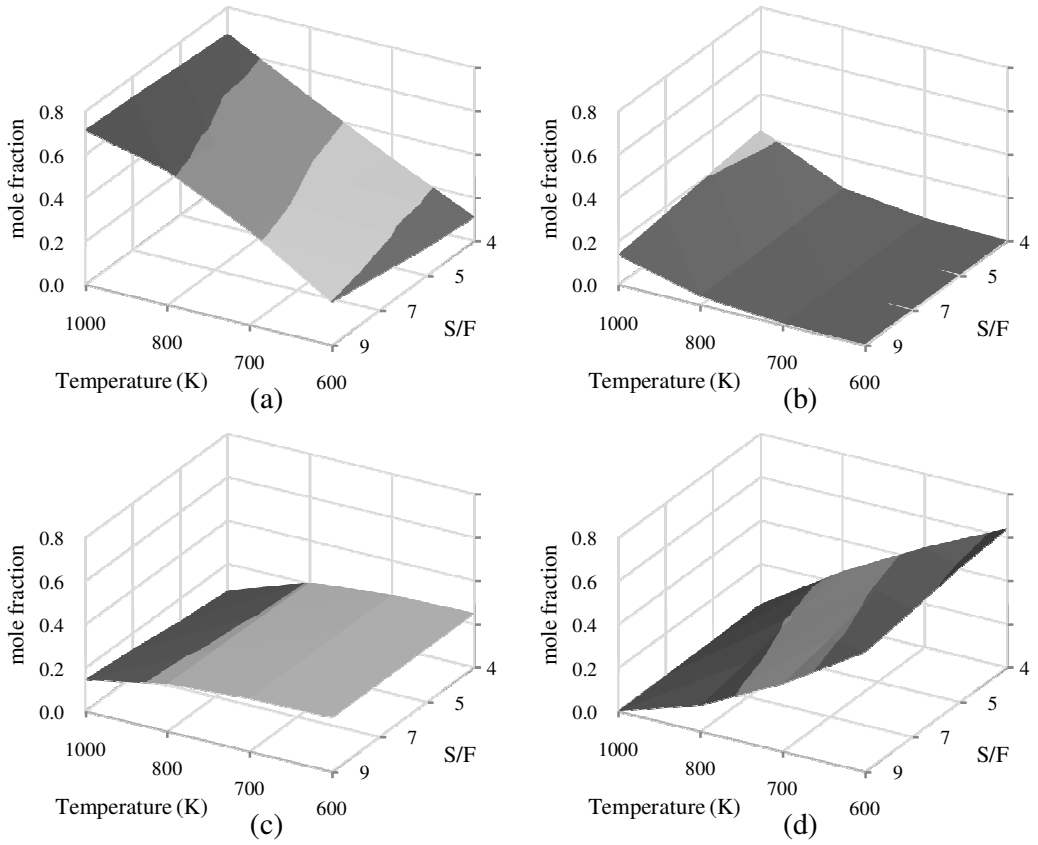

Figure 4.2. Effects of temperature and steam to fuel ratio on the mole fractions of the products during Isopropyl Alcohol conversion (dry basis, 1 bar) (a) H_2, (b) CO, (c) CO_2, (d) CH_4

The change of mole fraction of methane with temperature, given in Figure 4.2d, provides further data about the nature of the possible reactions. As in the case of formic acid, CH_4 production is favored with decreasing temperatures and is at its maximum level at the lowest value of the temperature range (600 K). When this observation is considered together with decreasing trends of hydrogen and CO at lower temperatures, it can be

concluded that methanation, Reaction (2.7), and its opposite, methane steam reforming, become significant as the temperature is reduced and is elevated, respectively.

Apart from temperature, the effect of steam-to-fuel ratio is also investigated. It is observed that, at 600 K, the increase in the amount of steam affects the product distribution via the methanation reaction, since mole fraction of CH_4 decrease and that of hydrogen increase as S/F ratio is elevated. However, at 1000 K, although not favored at high temperatures, the clear effect of WGS equilibrium is observed: feeding more steam has led to the increase of mole fractions of CO_2 and hydrogen from 0.075 to 0.146 (Figure 4.2c) and from 0.678 to 0.714 (Figure 4.2a), respectively, whereas mole fraction of CO is reduced from 0.233 to 0.139 (Figure 4.2b) The trend at 1000K also indicates that the concentration effect is dominant over the contradicting temperature effect in setting the direction of the WGS equilibrium.

When the two extremes of S/F ratios, 4 and 9, are compared, it can be seen that presence of high quantities of steam dampens the effect of RWGS and facilitates methane steam reforming. This observation is based on the fact that the rate of increase of mole fraction of hydrogen with temperature is higher at S/F=9 than found in S/F=4 (Figure 4.2a). Similarly, rate of increase of CO is lower and rates of decrease of CO_2 and CH_4 are lower and higher, respectively at S/F=9 (Figures 4.2b - 4.2d).

4.1.3. Lactic Acid

The third bio oil component that has been investigated for its steam reforming conversion to a hydrogen rich mixture is lactic acid. This conversion can be described via the following reaction:

$$C_3H_6O_3 + 3H_2O = 3CO_2 + 6H_2 \qquad \Delta H^o_{298} = 220.38 \text{ kJ/mol} \quad (4.4)$$

Results of the thermodynamic analysis of the steam-assisted conversion of lactic acid are given in Figure 4.3. In general, the results are comparable to those of isopropyl alcohol (Figure 4.2). The maximum value of hydrogen mole fraction is estimated as 0.625 at S/F=9 and at 1000 K (Figure 4.3a), whereas the equivalent value obtained in case of isopropyl

alcohol was 0.714. This point difference can be observed for the hydrogen mole fractions calculated in the whole range of steam-to-fuel and temperature values (Figures 4.2a and 4.3a). One other notable difference is in the levels of CO_2 production: lactic acid conversion seems to end up with mole fractions of CO_2 higher than obtained in isopropyl alcohol conversion (Figures 4.2c and 4.3c). These observations can be attributed to the differences in the stoichiometric coefficients of the reactions. Molar conversion of lactic acid gives 6 moles of hydrogen and 3 moles of CO_2, whereas the ratio of hydrogen to CO_2 in molar isopropyl alcohol conversion is 3 (i.e. Reaction (4.2)).

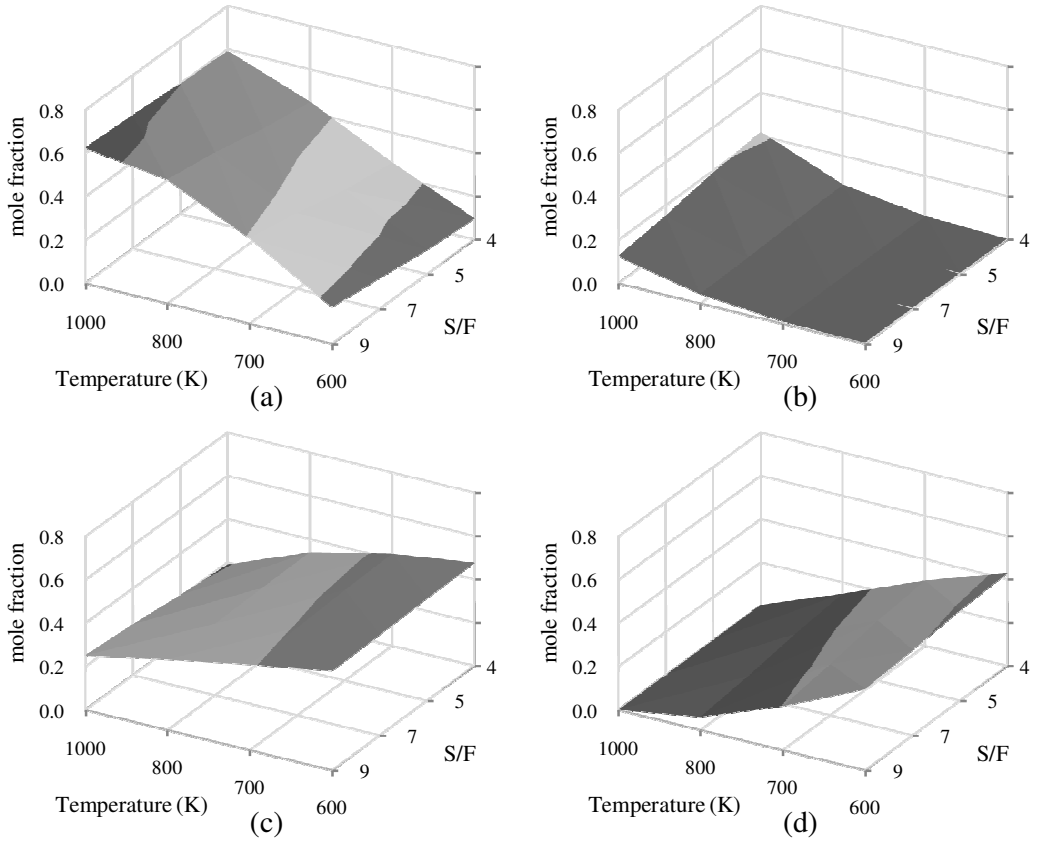

Figure 4.3. Effects of temperature and steam to fuel ratio on the mole fractions of the products during Lactic Acid conversion (dry basis, 1 bar) (a) H_2, (b) CO, (c) CO_2, (d) CH_4

The responses of the mole fractions of species against changes in temperature and steam-to-fuel ratio in lactic acid conversion are similar to the results obtained for isopropyl alcohol (Figures 4.2 and 4.3). At low temperatures, i.e. between 600 and 700 K, the

equilibrium mixture includes high amounts of CH_4 and CO_2 with negligible amount CO and a moderate amount of hydrogen. The possible reason of the low mole fractions of hydrogen is due to the dominance of the exothermic methanation, Reaction (2.7), which consumes H_2 with a higher stoichiometric relation relative to the CO. Under these conditions, increase in the S/F ratios facilitate the extent of reforming reaction in limited values and, therefore, shifts the equilibrium for producing more H_2 via both steam methane reforming, Reaction (2.1), and the WGS, (Reaction 2.2). Note that CO remains almost unchanged by the increase of S/F from 4 to 9 (at 600-700 K), since CO produced by steam reforming is most likely consumed by the water-gas shift (Figure 4.3b). In addition, increased S/F values favor the production of H_2 more than CO_2 due to additional hydrogen production via the methane reforming.

At high temperature region (between 700-1000 K) it can be observed that the elevation in temperature has led to the increased consumption of methane and increased production of hydrogen and CO. One other observation is that, at the 800-1000 K range, the rate of increase in the mole fraction hydrogen is dampened (Figure 4.3a) and the existence of CO_2 is lowered (Figure 4.3c). These observations indicate the significance of methane steam reforming as well as the RWGS, the latter being more dominant at the 800-1000 K range, as in the case of isopropyl alcohol. However, the same temperature range, elevation in the S/F ratio from 4 to 9 slightly triggers the water-gas shift effect, as observed by increased hydrogen and CO_2 and lowered CO fractions.

4.1.4. Phenol

Phenol is the hydrocarbon including the highest carbon number in this study. Conversion of phenol to hydrogen in the presence of steam can be described by the reactions given in Chapter 2 with Reaction (2.15) and (2.16).

Results of the thermodynamic analysis of phenol conversion are given in Figure 4.4, and, it can be seen that the molar compositions trends are similar to those of isopropyl alcohol and lactic acid. The endothermic natures of the reactions lead to a positive correlation between mole fraction of hydrogen and temperature at all S/F ratios, as expected (Figure 4.4a). At low temperatures (e.g. 600 K), the presence of CH_4 can be

attributed to the exothermic nature of the methanation, Reaction (2.7), and the dominance of CO_2 to CO can be explained by the lower enthalpy of Reaction (2.15). One other explanation of the carbon oxide distribution can be made by the WGS effect: When the WGS reaction, Reaction (2.2), is multiplied by a coefficient of 6 and is added to Reaction (2.16), Reaction (2.2) can be obtained. In other words, the clear dominance of the exothermic WGS at low temperatures leads to the immediate conversion of CO formed by Reaction (2.16) to CO_2.

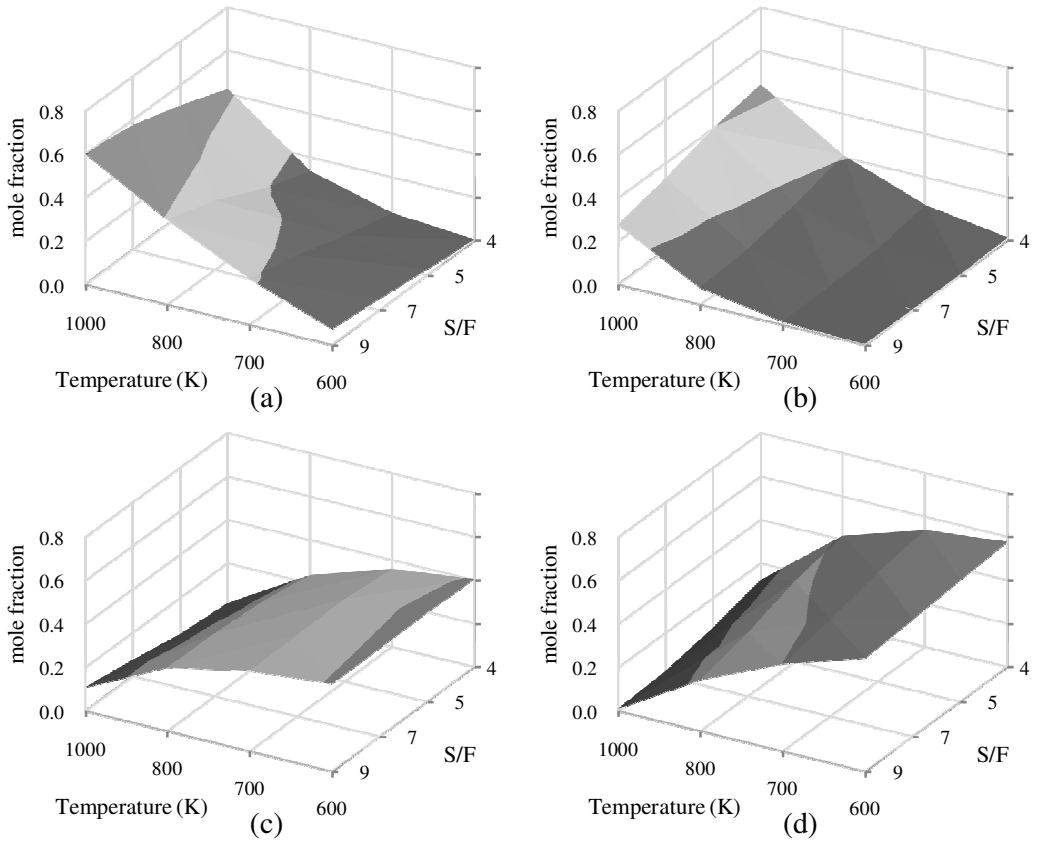

Figure 4.4. Effects of temperature and steam to fuel ratio on the mole fractions of the products during Phenol conversion (dry basis, 1 bar) (a) H_2, (b) CO, (c) CO_2, (d) CH_4

When the temperature is increased, the formation of H_2 and CO is favored with decreasing quantities of CO_2 and CH_4 (Figure 4.4). The change in S/F ratio also gave similar responses with the other hydrocarbons; hydrogen and CO_2 production are positively affected, whereas the amounts of CO and CH_4 are found to decline with the

presence of increased quantities of steam. However, although trends do match with each other, the magnitude of the responses against changes in process conditions – temperature and steam-to-fuel ratio – is higher in case of phenol. This is thought to be due to the high values of the stoichiometric coefficients, resulting from the high carbon number of phenol. To illustrate, one mole of phenol gives 6 moles of CO and 8 moles of hydrogen via Reaction (2.16), 3 moles of CO and 6 moles of hydrogen are produced by steam reforming of isopropyl alcohol (Reaction 4.3). This would in turn cause the changes in the mole fractions to be more significant (Figures 4.2 and 4.4).

4.2. Results of Thermodynamic Analysis at 30 bar

Determination of the molar distribution of the components at 30 bar is more complicated than the cases where total pressure was equal to 1 bar (Section 4.1) in the sense that the former requires the simulation of a non-ideal gas behavior and involves the use of Soave Redlich-Kwong (SRK) equation of state for evaluating fugacity coefficients and for adding the pressure effect into the product distribution at equilibrium.

4.2.1. Formic Acid

Results of the thermodynamic analysis of steam-assisted formic acid conversion at 30 bar are given in Figure 4.5. When compared with the outcomes of 1 bar simulations, it can be observed that the changes in the product distribution and sensitivity of the product distribution against S/F and temperature are not significantly affected (Figure 4.1 and 4.5). Table 4.1 shows the deviations of the dry basis mole fractions from the 1 bar to 30 bar. For example, at S/F=4 and at T=600K, the difference of the mole fraction of hydrogen evaluated at 30 bar and at 1 bar is equal to –0.1487. It is clearly seen that for the high-pressure formic acid reactions, the hydrogen content is decreased as the pressure is increased. The greatest difference is obtained at 700 K with S/F = 9. The formations of CH_4 and CO_2, on the other hand, are found to increase with pressure (Table 4.1).

As mentioned above, high pressure favors the conversion of hydrogen. This is expected since formic acid dehydrogenation, Reaction (4.1), produces 2 moles of products with 1 mole of reactant. In other words, when temperature is kept constant, due to the Le

Chatelier's principle, equilibrium will shift in the direction of lower total volume, i.e. lower number of moles, which will lead to decrease in mole fraction of hydrogen (Table 1). The same principle would result in the decrease of CO_2 mole fractions, but the opposite is observed in (Table 1). This can be explained by increasing quantities of methane at high pressures; positive deviations in Table 1 and comparison of Figures 4.5d and 4.1d clearly show that the rate of decrease of mole fraction of CH_4 is lower at 30 bar. This effect is due to the methanation reaction, Reaction (2.7), which is favored in the direction of methane formation at high pressures due to reduction of total number of moles from 4 to 2. The stoichiometry of methanation dictates consumption of hydrogen to be three times higher than that of CO; hydrogen will be removed faster than the CO. When this is considered in the context of water-gas shift, a reaction running simultaneously, the balance will shift in the direction of CO_2 and H_2 formation, and, therefore, the amount of CO_2 will tend to increase.

Table 4.1. Deviations of the mole fractions of the products of Formic Acid conversion from 1 bar to 30 bar (dry-basis)

		Temperature (K)						Temperature (K)			
	S/F	600	700	800	1000		S/F	600	700	800	1000
H_2	4	-0.1487	-0.2766	-0.2325	-0.0186	CO	4	-0.0009	-0.0061	-0.0135	-0.0004
	5	-0.1702	-0.2883	-0.2097	-0.0118		5	-0.0008	-0.0053	-0.0098	0.0011
	7	-0.2067	-0.2953	-0.1677	-0.0055		7	-0.0007	-0.0040	-0.0053	0.0020
	9	-0.2364	-0.2889	-0.1331	-0.0031		9	-0.0007	-0.0031	-0.0029	0.0020
CO_2	4	0.0750	0.1429	0.1264	0.0096	CH_4	4	0.0746	0.1398	0.1196	0.0094
	5	0.0857	0.1481	0.1122	0.0050		5	0.0853	0.1455	0.1073	0.0056
	7	0.1039	0.1507	0.0878	0.0012		7	0.1035	0.1487	0.0852	0.0022
	9	0.1187	0.1467	0.0687	0.0000		9	0.1184	0.1452	0.0673	0.0010

The reaction mechanism above can be further validated by the effect of temperature. Water-gas shift and methanation are exothermic reactions and are less favored at higher temperatures. This principle can explain the reduced deviations of CH_4 and CO_2 at high temperatures and, it can be observed that the pressure effect is almost balanced by the opposing temperature effect at 1000 K (Table 4.1).

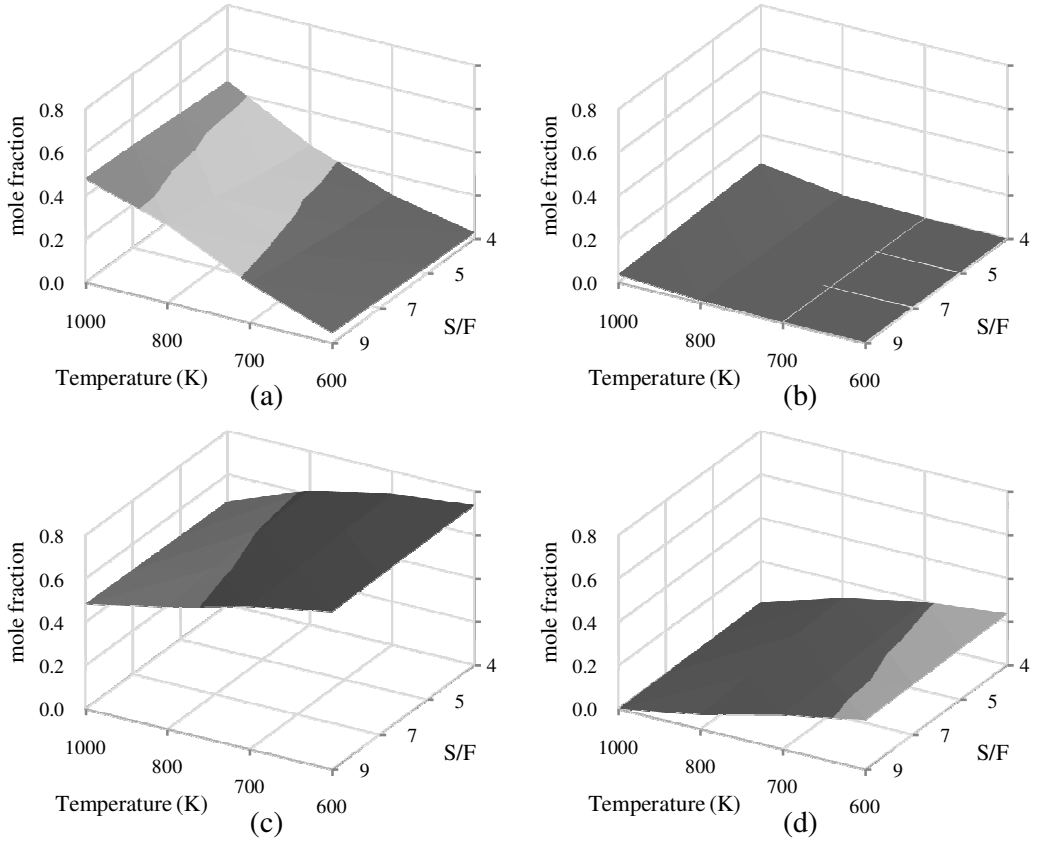

Figure 4.5. Effects of temperature and steam to fuel ratio on the mole fractions of the products during Formic Acid conversion (dry basis, 30 bar) (a) H_2, (b) CO, (c) CO_2, (d) CH_4

The effect of steam-to-fuel ration on the product distribution helps in further clarification of the significance of the reactions. Results in Table 1 show that, the direction of the deviations in H_2, CO_2 and CH_4 mole fractions change at 700 K. To illustrate, deviations in hydrogen mole fractions are –0.2883, -0.2953 and –0.2889 at S/F ratios of 5, 7 and 9, respectively, i.e. the maximum deviation occurs at S/F=7. The deviations start to decline after this point, and eventually ends up with –0.0031 at S/F=9 and at 1000 K. The same trend can be observed for CO_2 and CH_4. Apart from these, the deviations in CO mole fractions are found to increase with S/F ratios. These results indicate that methane steam reforming starts to compete with its opposite, methanation reaction, as of 700 K, and becomes more dominant at higher steam-to-fuel ratios.

4.2.2. Isopropyl Alcohol

Results of the thermodynamic analysis of steam-assisted conversion of isopropyl alcohol at 30 bar are given in Figure 4.6 and in Table 4.2. The trends of the responses of product distributions against temperature and steam-to-fuel ratio are similar to those calculated at 1 bar (Figures 4.2 and 4.6). However, the most important difference is with the mole fraction of methane, which is found to be almost zero at 1000 K, whereas it is higher than 0.1 depending on the steam-to-fuel ratio (Figures 4.2d and 4.6d). These results and the positive deviations obtained for methane in Table 4.2 demonstrate the influence of methanation reaction. Moreover, comparison of the CH_4 deviations obtained for formic acid and isopropyl alcohol shows that the magnitude of the effect of pressure increase is higher in the latter hydrocarbon (Tables 4.1 and 4.2), which might be due to the higher amounts of hydrogen and carbon monoxide converted.

Table 4.2. Deviations of the mole fractions of the products of Isopropyl Alcohol conversion from 1 bar to 30 bar (dry-basis)

		Temperature (K)						Temperature (K)			
	S/F	600	700	800	1000		S/F	600	700	800	1000
H_2	4	-0.0901	-0.2166	-0.3092	-0.4448	CO	4	-0.0007	-0.0086	-0.0468	-0.0929
	5	-0.1067	-0.2426	-0.3239	-0.3212		5	-0.0006	-0.0079	-0.0421	-0.0904
	7	-0.1365	-0.2906	-0.3369	-0.1713		7	-0.0005	-0.0078	-0.0357	-0.0776
	9	-0.1627	-0.3084	-0.3382	-0.1383		9	-0.0005	-0.0064	-0.0313	-0.0571
CO_2	4	0.0005	0.0064	0.0351	0.0696	CH_4	4	0.0903	0.2187	0.3209	0.4680
	5	0.0004	0.0059	0.0315	0.0678		5	0.1069	0.2445	0.3344	0.3437
	7	0.0004	0.0058	0.0267	0.0582		7	0.1366	0.2925	0.3458	0.1906
	9	0.0003	0.0048	0.0234	0.0428		9	0.1628	0.3099	0.3459	0.1526

The stoichiometry of isopropyl steam reforming reactions (4.2) and (4.3) indicate that formation of hydrogen, CO and CO_2 are not favored at high pressures due to Le Chatelier's principle. This principle can explain the negative deviations that occurred in the mole fractions of hydrogen and CO (Table 4.2). It is also worth noting that the impact of pressure increase on hydrogen is much higher than in CO; this might be linked due to the individual stoichiometric coefficients of these molecules in reactions (4.2) and (4.3). The contradictory response of CO_2, on the other hand, can be linked to the faster removal of

hydrogen than CO by reverse of Reaction (4.2) and by methanation, Reaction (2.7), which in turn facilitates the CO_2 production by the water-gas shift.

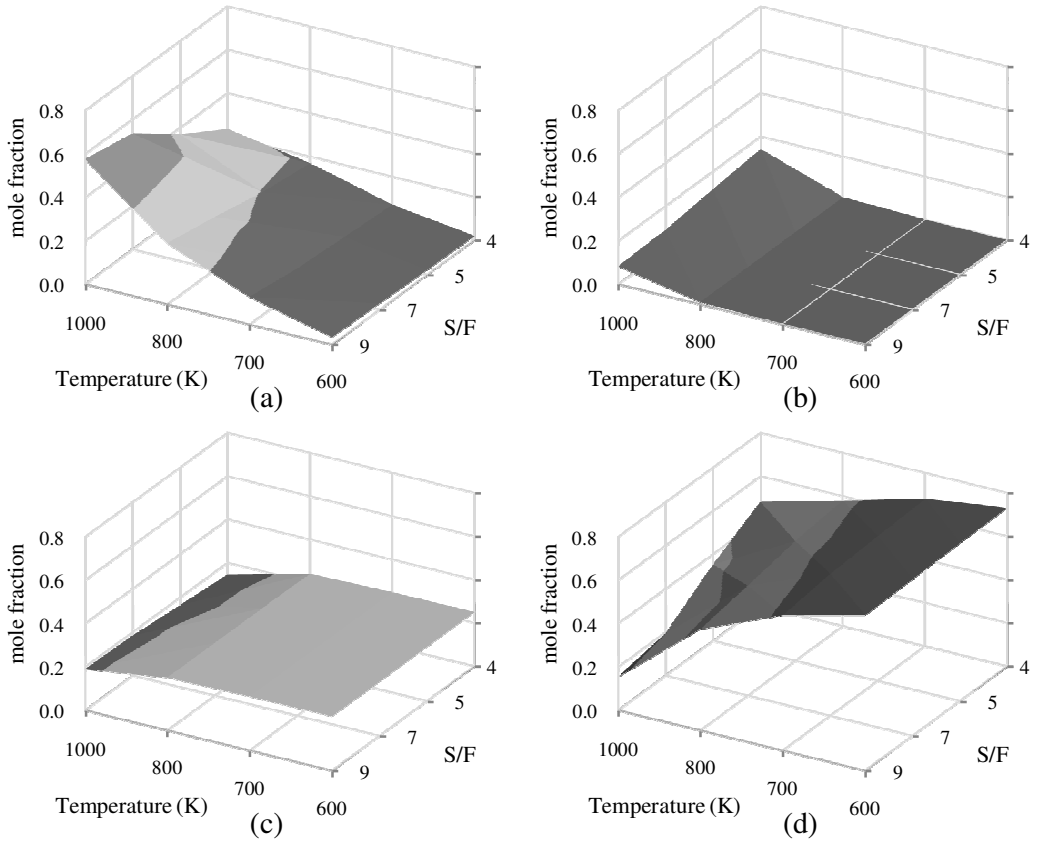

Figure 4.6. Effects of temperature and steam to fuel ratio on the mole fractions of the products during Isopropyl Alcohol conversion (dry basis, 30 bar) (a) H_2, (b) CO, (c) CO_2, (d) CH_4

The effect of steam-to-fuel ratio can be notable only at 1000 K, since the opposing effect of pressure on the methane and isopropyl alcohol steam reforming is thermodynamically balanced at high temperatures. Figures 4.6a and 4.6d show that increase in the S/F ratio facilitates hydrogen production and removal of methane only at 1000 K. The significance of steam reforming at this temperature is also verified by existence of CO (Figure 4.6b). The slight increase of mole fraction of CO2 by the presence of steam at 1000 K also indicates the limited progress of Reaction (4.2).

4.2.3. Lactic Acid

Results of the thermodynamic analysis of steam-assisted conversion of lactic acid at 30 bar are given in Figure 4.7 and in Table 4.3. In general, the trends observed in the product distributions (Figures 4.3 and 4.7) and in the pressure-induced deviations and the reasoning behind them are similar to what have been observed and proposed in isopropyl alcohol steam reforming (Section 4.2.2, Figures 4.6 and 4.7). However, one difference can be observed in the magnitudes of the deviations, which show that the values obtained in lactic acid steam reforming are generally lower than those obtained in the case of isopropyl alcohol (Tables 4.2 and 4.3). This can be explained by comparing the stoichiometry of Reactions (4.2) and (4.4). The difference in the number of moles of reactants and products of isopropyl alcohol and lactic acid steam reforming are 6 and 4, respectively. Therefore, it can be claimed that the lower value of the difference in the latter dampens the effect of pressure increase on the product distribution.

Table 4.3. Deviations of the mole fractions of the products of Lactic Acid conversion from 1 bar to 30 bar (dry-basis)

		Temperature (K)						Temperature (K)			
	S/F	600	700	800	1000		S/F	600	700	800	1000
H_2	4	-0.0792	-0.2018	-0.3017	-0.1899	CO	4	-0.0011	-0.0108	-0.0502	-0.0867
	5	-0.0928	-0.2254	-0.3154	-0.1668		5	-0.0010	-0.0099	-0.0443	-0.0696
	7	-0.1180	-0.2626	-0.3286	-0.1295		7	-0.0009	-0.0086	-0.0360	-0.0459
	9	-0.1408	-0.2901	-0.3301	-0.1014		9	-0.0009	-0.0077	-0.0301	-0.0309
CO_2	4	0.0206	0.0586	0.1131	0.1125	CH_4	4	0.0597	0.1541	0.2388	0.1641
	5	0.0240	0.0638	0.1121	0.0939		5	0.0699	0.1715	0.2477	0.1425
	7	0.0302	0.0721	0.1091	0.0668		7	0.0887	0.1991	0.2554	0.1086
	9	0.0359	0.0783	0.1051	0.0485		9	0.1058	0.2195	0.2551	0.0838

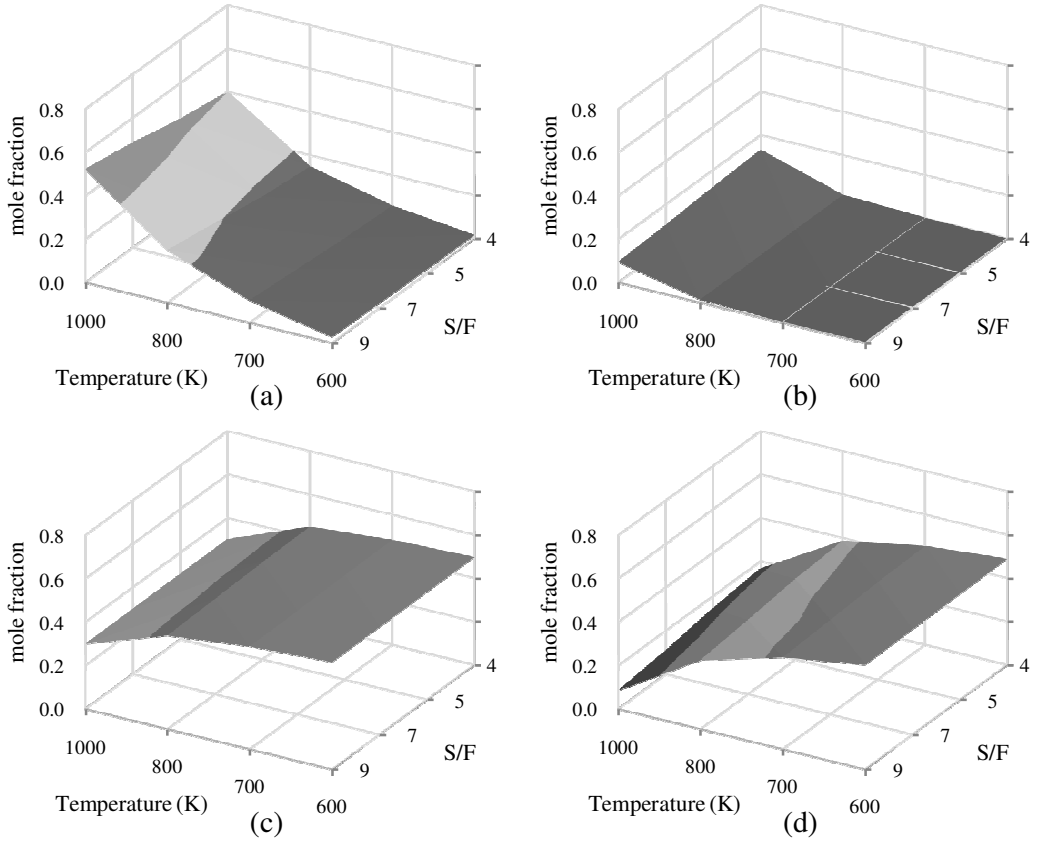

Figure 4.7. Effects of temperature and steam to fuel ratio on the mole fractions of the products during Lactic Acid conversion (dry basis, 30 bar) (a) H_2, (b) CO, (c) CO_2, (d) CH_4

4.2.4. Phenol.

Results of the thermodynamic analysis of steam-assisted conversion of phenol at 30 bar are given in Figure 4.8 and in Table 4.4. As in the case of other hydrocarbons, the 1-bar and 30-bar trends are comparable to each other (Figures 4.4 and 4.8). However, the magnitudes of the pressure-induced deviations of the mole fractions are smaller in case of phenol steam reforming than in the case of other hydrocarbons (Table 4.4). The effect of pressure can be observed at the 600-700 K range, but fades out at higher temperatures. This might be the due to the property of the component such that optimizations conducted at high temperatures give compressibility factors close to 1 and this can make the solutions similar to the ideal gas (1 bar) results as shown in Table 4.5.

Table 4.4. Deviations of the mole fractions of the products of Phenol conversion from 1 bar to 30 bar (dry-basis)

		Temperature (K)						Temperature (K)			
	S/F	600	700	800	1000		S/F	600	700	800	1000
H_2	4	-0.0009	-0.0066	0.0000	0.0000	CO	4	-0.0028	-0.0136	0.0000	0.0000
	5	-0.0054	-0.0165	0.0000	0.0000		5	-0.0005	-0.0054	0.0000	0.0000
	7	-0.0100	-0.0277	0.0000	0.0000		7	-0.0003	-0.0032	0.0000	0.0000
	9	-0.0136	-0.0347	-0.0516	-0.0051		9	-0.0003	-0.0025	-0.0103	-0.0004
CO_2	4	0.0022	0.0113	0.0000	0.0000	CH_4	4	0.0015	0.0089	0.0000	0.0000
	5	0.0013	0.0068	0.0000	0.0000		5	0.0046	0.0151	0.0000	0.0000
	7	0.0019	0.0070	0.0000	0.0000		7	0.0084	0.0238	0.0000	0.0000
	9	0.0025	0.0077	0.0163	0.0011		9	0.0114	0.0296	0.0456	0.0044

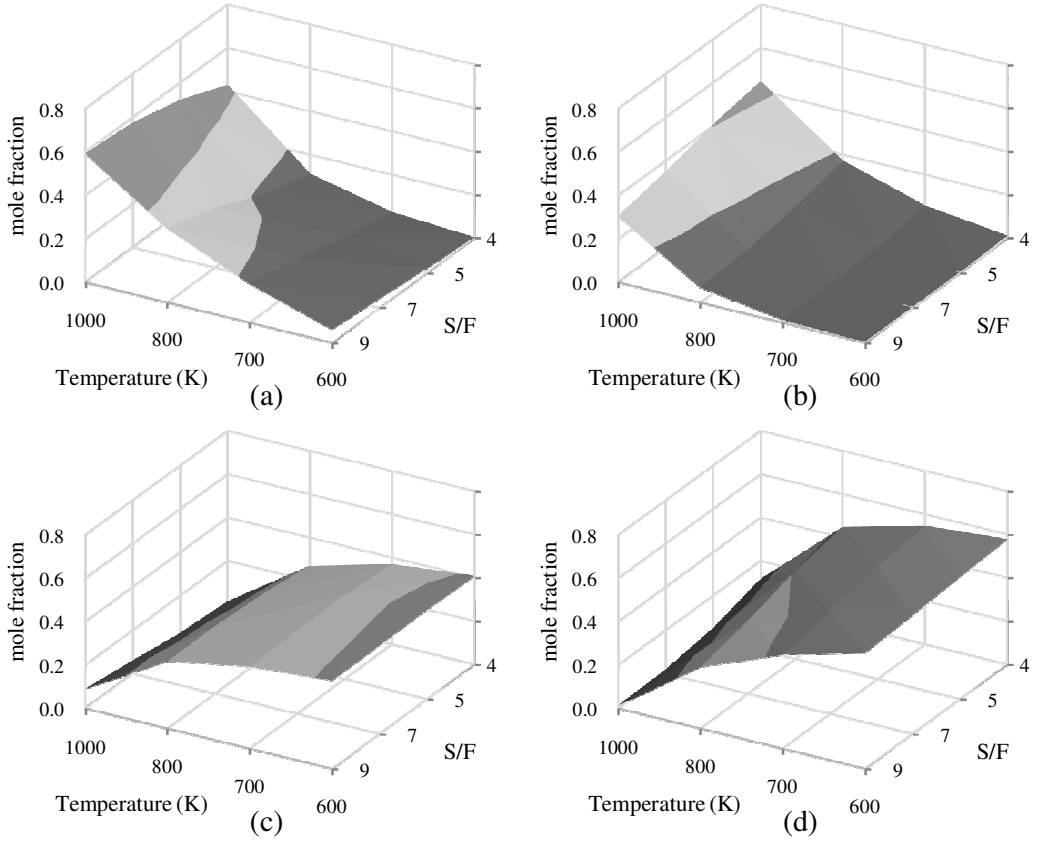

Figure 4.8. Effects of temperature and steam to fuel ratio on the mole fractions of the products during Phenol conversion (dry basis, 30 bar) (a) H_2, (b) CO, (c) CO_2, (d) CH_4

Table 4.5 gives the number of moles and compressibility factors calculated for phenol steam reforming at 30 bar. The results indicate that when the temperature is lowered the system starts to deviate from the ideal conditions, which can be observed by the reduced values of compressibility factors at lower temperatures. In addition, increase in the steam-to-fuel ratio has led to the slight decrease of compressibility factors (e.g. at 600 K, z=0.939 and 0.960 at S/F of 9 and 7, respectively). These findings can be helpful in explaining the deviation trends observed in Table 4.4.

Table 4.5. Number of moles and compressibility factors obtained for steam reforming of phenol at 30 bar

	T = 600 K			S/F = 9			
S/F and T (K)	4	5	7	600	700	800	1000
C_6H_6O	0.000	0.000	0.000	0.000	0.000	0.000	0.000
H_2	0.022	0.137	0.270	0.386	1.303	3.103	8.750
H_2O	0.023	0.938	2.869	4.811	4.394	3.758	2.873
CO	0.068	0.013	0.009	0.007	0.092	0.618	4.495
CO_2	2.455	2.524	2.561	2.591	2.757	2.812	1.316
CH_4	3.477	3.462	3.430	3.402	3.151	2.570	0.189
z	0.960	0.969	0.960	0.939	0.978	0.997	1.000
G_t(kJ)	-98.69	-1197.94	-1606.72	-2011.27	-1924.33	-1832.86	-1652.67

5. CONCLUSIONS AND RECOMMENDATIONS

5.1. Conclusions

The aim of the study is to perform a thermodynamic analysis of bio oil components, – formic acid, isopropyl alcohol, lactic acid and phenol – and to understand the effect of the temperature, pressure and inlet steam-to-fuel ratio on the product distribution. The thermodynamic analysis is performed at range of temperature, pressure and steam-to-fuel ratio of 600–1000 K, 1–30 bar and 4–9, respectively and the number of moles of each component in the product stream at equilibrium are calculated. The main results of the thesis are listed as follows:

- All the model hydrocarbons are almost completely converted to H_2, CO, CO_2 and CH_4 under the range of operating conditions examined.

- At constant steam-to-fuel ratios and pressures, increase in the temperature has led to significant increase in the mole fraction of hydrogen, coinciding with the endothermic feature of the steam reforming reactions. A small difference is observed for formic acid in the sense that maximum hydrogen is obtained at 800 K, which is most likely due to the production of hydrogen by exothermic dehydrogenation of formic acid.

- The sensitivity of the product distributions against changes in the operating conditions indicate the presence of water-gas shift/reverse water-gas shift and methanation/methane steam reforming as major side reactions of the system.

- Increased steam-to-fuel ratio ends up with higher hydrogen and carbon dioxide quantities and reduces amounts of carbon monoxide and methane. This effect is found to be more significant at low temperatures

- High-pressure operation has given lower hydrogen and carbon monoxide content while increase in methane and carbondioxide is observed for all operation ranges, which are consistent with the stoichiometry of the possible side reactions

- The optimization in SQP with ideal gas assumption is very simple and quick while the real gas counterpart introduced the nonlinearity both in the objective function and in the constraint. These bring difficulties in terms of being robust, i.e. reaching the global optimum without boundaries representing the physical limitations.

5.2. Recommendations

The recommendations we deduce from the study may be summarized as follows:

- Thermodynamic analysis can be improved (a) by including the presence of liquid phase, (b) by implementing higher number of possible products into the calculations and (c) by taking the possibility of solid carbon formation into account.

- Other bio oil based component can be investigated for the efficiency of hydrogen production via thermodynamic analysis.

APPENDIX

Table A.1. Gibbs Free Energy of Formation (J/mol) of Selected Hydrocarbons (CRC Handbook, 1985)

T (K)	CH_2O_2	C_3H_8O	$C_3H_6O_3$	C_6H_6O
600	-330171.0	-67156.3	-387320.9	36650.0
700	-319829.7	-29642.5	-347797.5	60750.0
800	-309362.7	8164.3	-308064.7	85020.0
1000	-288177.4	84364.0	-228306.2	134280.0

Table A.2. Gibbs Free Energy of Formation (J/mol) of Products (CRC Handbook, 1985)

T (K)	H_2	H_2O	CO	CO_2	CH_4
600	0.0	-214008.0	-164480.0	-395152.0	-22690.0
700	0.0	-208814.0	-173513.0	-395367.0	-12476.0
800	0.0	-203501.0	-182494.0	-395558.0	-1993.0
1000	0.0	-192603.0	-200281.0	-395865.0	19475.0

Table A.3. Gibbs Free Energy of Formation (J/mol) of Possible Hydrocarbon-based Side Products in (Allendorf, 2007)

T (K)	C_2H_2	C_2H_4	C_2H_6	C_3H_4	C_3H_6
600	192454.0	87982.0	26086.0	212605.7	162089.0
700	186823.0	95434.0	46800.0	217211.2	182583.0
800	181267.0	103142.0	67887.0	222109.7	203404.0
1000	170355.0	119067.0	110750.0	232451.1	245618.0
T (K)	C_3H_8	C_5H_4	C_5H_6	C_5H_8	C_6H_6
600	64961.0	461720.3	317233.8	233539.7	182680.0
700	96065.0	461511.0	328998.7	259121.1	201590.0
800	127603.0	461511.0	341224.2	285246.7	220820.0
1000	191444.0	462139.0	366721.8	338586.5	259890.0

Table A.4. Thermodynamic Critical Constants of Selected Hydrocarbons (Reid et al.,c1987)

	CH_2O_2	C_3H_8O	$C_3H_6O_3$	C_6H_6O	H_2	H_2O	CO	CO_2	CH_4
T_c (K)	588.0	508.3	604.0	694.3	33.2	647.3	132.9	304.1	190.4
P_c (bar)	58.1	47.6	58.2	61.3	13.0	221.3	35.0	73.8	46.0
w	0.317	0.669	0.334	0.426	-0.218	0.344	0.066	0.239	0.111

REFERENCES

Adhikari, S., S. Fernando, S. R. Gwaltney, S. D. F. To, R. M Bricka, P. Steele and A. Haryanto, 2007, "Athermodynamic analysis of hydrogen production by steam reforming of glycerol", *International Journal of Hydrogen Energy*, Vol. 32, pp. 2875 – 2880.

Allendorf, M., 2007, *Sandia National Laboratories, Thermodynamic Resource – Gas Phase Database*, http://public.ca.sandia.gov/HiTempThermo/mp4search.html

Armor, J. N., 1999, "The Multiple Roles for Catalysis in the Production of H_2", *Applied Catalysis A: General*, Vol. 176, pp. 159-176.

Avcı, A. K., D. L. Trimm, A. E. Aksoylu and Z. I. Önsan, 2004, "Hydrogen production by steam reforming of n-butane over supported Ni and Pt-Ni catalysts", *Applied Catalysis A: General*, Vol. 258, pp. 235–240.

Avcı, A. K., Z. I. Önsan and D. L. Trimm, 2001, "On-board fuel conversion for hydrogen fuel cells: comparison of different fuels by computer simulations", *Applied Catalysis A: General*, Vol. 216, pp. 243–256.

Balasubramanian, B., A. L. Ortiz, S. Kaytakoglu and D. P. Harrison, 1999, "Hydrogen from methane in a single-step process", *Chemical Engineering Science*, Vol. 54, pp. 3543 – 3552.

Barelli, L., G. Bidini, F. Gallorini and S. Servili, 2008, "Hydrogen production through sorption-enhanced steam methane reforming and membrane technology: A review", *Energy*, Vol. 33, pp. 554–570.

Basagiannis, A. C. and X. E. Verykios, 2007, "Catalytic steam reforming of acetic acid for hydrogen production", *International Journal of Hydrogen Energy*, Vol. 32, pp. 3343 – 3355.

Bimbela, F., M. Oliva, J. Ruiz, L. Garcı´a and J. Arauzo, 2000, "Hydrogen production by catalytic steam reforming of acetic acid, a model compound of biomass pyrolysis liquids", *J. Anal. Appl. Pyrolysis*, Vol. 79, pp. 112–120.

Elliott L., D. B. Ingham, A.G. Kyne, N. S. Mera, M. Pourkashanian and C. W. Wilson, 2000, "Genetic algorithms for optimisation of chemical kinetics reaction mechanisms", *Progress in Energy and Combustion Science*, Vol. 30, Issue 3, pp. 297-328.

Esposito, W. R. and C. A. Floudas, 2000, "Deterministic Global Optimization in Nonlinear Optimal Control Problems", *Journal of Global Optimization*, Vol. 17, pp. 97–126.

Faungnawakij, K., R. Kikuchi and K. Eguchi, 2006, "Thermodynamic evaluation of methanol steam reforming for hydrogen production", *Journal of Power Sources*, Vol. 161, pp. 87–94.

Fishtik, I., A. Alexander, R. Datta, and D. Geana, 2000, "A thermodynamic analysis of hydrogen production by steam reforming of ethanol via response reactions", *International Journal of Hydrogen Energy*, Vol. 25, pp. 31 – 45.

Floudas, C. A., 1997, "Deterministic global optimization in design, control and computational chemistry", *Institute for Mathematics and Its Applications*, Vol. 93, pp. 129.

Floudas, C. A., 2000, *Deterministic global optimization: theory, methods, and applications*, Kluwer Academic Publishers, Boston.

Floudas, C. A., I. G. Akrotirianakis, S. Caratzoulas, C. A. Meyer and J. Kallrath, 2005, "Global optimization in the 21st century: Advances and challenges, "*Computers and Chemical Engineering*, Vol. 29, pp. 1185–1202.

Gill, P. E., W. Murray, M. A. Saunders, A. Drud, E. Kalvelagen, 2002, "GAMS/SNOPT: An SQP Algorithm for Large-Scale Constrained Optimization" *The Solver Manuals*, May 10.

Harding, S. T. and C. A. Floudas, 2000, "Journal Phase Stability with Cubic Equations of State: Global Optimization Approach", *AIChE*, Vol. 46, No. 7, pp. 1422 – 1440, July.

Iojoiu, E. E., M. E. Domine, T. Davidian, N. Guilhaume and C. Mirodatos, 2007, "Hydrogen production by sequential cracking of biomass-derived pyrolysis oil over noble metal catalysts supported on ceria-zirconia", *Applied Catalysis A: General*, Vol. 323, pp. 147–161.

Ishihara, A., E. W. Qian, I. N. Finahari, I. P. Sutrisna and T. Kabe, 2005, "Addition effect of ruthenium on nickel steam reforming catalysts", *Fuel*, Vol. 84, pp. 1462–1468.

Joensen, F. and J. R. Rostrup-Nielsen, 2002, "Conversion of hydrocarbons and alcohols for fuel cells", *Journal of Power Sources*, Vol. 105, pp. 195–201.

Kechagiopoulos, P. N., S. S. Voutetakis, A. A. Lemonidou and I. A. Vasalos, 2007, "Sustainable hydrogen production via reforming of ethylene glycol using a novel spouted bed reactor", *Catalysis Today*, Vol. 127, pp. 246–255.

Laosiripojana, N. and S. Assabumrungrat, 2006, "Hydrogen production from steam and autothermal reforming of LPG over high surface area ceria", *Journal of Power Sources*, Vol. 158, pp. 1348–1357.

Lasdon, L., 2001, "Nonlinear and Geometric Programming – Current Status", *Annals of Operations Research*, Vol. 105, pp. 99–107.

Luo, N., F. Cao, X. Zhao, T. Xiao and D. Fang, 2007,, "Thermodynamic analysis of aqueous-reforming of polylols for hydrogen generation", *Fuel*, Vol. 86, pp. 1727–1736.

Lutz, A. E., R. W. Bradshaw, J. O. Keller and D. E. Witmer, 2003, "Thermodynamic analysis of hydrogen production by steam reforming", *International Journal of Hydrogen Energy*, Vol. 28, pp. 159 – 167.

Lwin,Y., W. R. W. Daud, A. B. Mohamad and Z. Yaakob, 2000, "Hydrogen production from steam-methanol reforming: thermodynamic analysis", *International Journal of Hydrogen Energy*, Vol. 25, pp. 47 – 53.

Mahishi, M. R. and D. Y. Goswami, 2007, "Thermodynamic optimization of biomass gasifier for hydrogen production", *International Journal of Hydrogen Energy*, Vol. 32, pp. 3831 – 3840.

Mansoornejad, B., N. Mostoufi and F. Jalali-Farahani, 2008, "A hybrid GA–SQP optimization technique for determination of kinetic parameters of hydrogenation reactions", *Computers and Chemical Engineering*, Vol. 32, pp. 1447–1455.

Marquevich, M., S. Czernik, E. Chornet and D. Montane, 1999, "Hydrogen from Biomass: Steam Reforming of Model Compounds of Fast-Pyrolysis Oil", *Energy & Fuels*, Vol. 13, pp. 1160 – 1166.

Mas, V., R. Kipreos, N. Amadeo and M. Laborde, 2006, "Thermodynamic analysis of ethanol/water system with the stoichiometric method", *International Journal of Hydrogen Energy*, Vol. 31, pp. 21 – 28.

McDonald, C. M. and C. A Floudas, 1994, "Global optimization for the phase and chemical equilibrium problem: application to the NRTL equation", *Computers & Chemical Engineering*, Vol 19, Issue 11, pp. 1111-1139.

Mizuno, T., Y. Matsumura, T. Nakajima and S. Mishima, "Effect of support on catalytic properties of Rh catalysts for steam reforming of 2-propanol", 2003, *International Journal of Hydrogen Energy*, Vol. 28, pp. 1393 – 1399.

Ni, M., D. Y. C. Leung, M. K. H. Leung and K. Sumathy, 2006, "An overview of hydrogen production from biomass", *Fuel Processing Technology*, Vol. 87, pp. 461 – 472.

Nichita, D.V., S. Gomez and E. Luna, 2002, "Multiphase equilibria calculation by direct minimization of Gibbs free energy with a global optimization method", *Computers and Chemical Engineering*, Vol. 26, pp. 1703 – 1724.

Nocedal, J. and S. Wright., c1999, *Numerical optimization*, New York : Springer.

Polychronopoulou, K., J. L. fG. Fierro, and A.M. Efstathiou, 2004, "The phenol steam reforming reaction over MgO-based supported Rh catalysts", *Journal of Catalysis*, Vol. 228, pp. 417 –432.

Rakass S., H. Oudghiri-Hassani, P. Rowntree and N. Abatzoglou, 2006, "Steam reforming of methane over unsupported nickel catalysts", *Journal of Power Sources*, Vol. 158, pp. 485–496.

Rangaiah, G. P., 2001, "Evaluation of genetic algorithms and simulated annealing for phase equilibrium and stability problems", *Fluid Phase Equilibria*, Vol. 187–188, pp. 83–109.

Reid, R C., J. M. Prausnitz and B. E. Poling, c1987, "The properties of gases and liquids", McGraw-Hill, New York.

Resini, C., L. Arrighi, M. C. H. Delgado, M. A. L. Vargase, L. J. Alemanye, P. Rianic, S. Berardinellia, R. Marazzac and G. Buscaa, 2006, "Production of hydrogen by steam reforming of C3 organics over Pd–Cu/□-Al_2O_3 catalyst", *International Journal of Hydrogen Energy*, Vol. 31, pp. 13 – 19.

Rioche, C., S. Kulkarni, F. C. Meunier, J. P. Breen and R. Burch, 2005, "Steam reforming of model compounds and fast pyrolysis bio-oil on supported noble metal catalysts", *Applied Catalysis B: Environmental*, Vol. 61, pp. 130–139.

Rostrup-Nielsen, J. R., 1984, "Sulfur-passivated nickel catalysts for carbon-free steam reforming of methane", *Journal of Catalysis*, Vol. 85, Issue 1, pp. 31-43, January.

Sandler, S., I., c1989, "*Chemical and engineering thermodynamics*", Wiley, New York.

Semelsberger, T. A. and R. L. Borup, 2005, "Thermodynamic equilibrium calculations of dimethyl ether steam reforming and dimethyl ether hydrolysis", *Journal of Power Sources*, Vol. 152, pp. 87–96.

Seo, Y. S., A Shirley and S. T. Kolaczkowski, 2002, "Evaluation of thermodynamically favourable operating conditions for production of hydrogen in three different reforming technologies", *Journal of Power Sources*, Vol. 108, pp. 213 – 225.

Swierczynski, D., C. Courson and A. Kiennemann, 2008, "Study of steam reforming of toluene used as model compound of tar produced by biomass gasification ", *Chemical Engineering and Processing*, Vol. 47, pp. 508 – 513.

Takanabe, K., K. Aika, K. Seshanb and L. Lefferts, 2004, "Sustainable hydrogen from bio-oil Steam reforming of acetic acid as a model oxygenate", *Journal of Catalysis*, Vol. 227, pp. 101–108

Vagia, E. C. and A. A. Lemonidou, 2007, "Thermodynamic analysis of hydrogen production via steam reforming of selected components of aqueous bio-oil fraction", *International Journal of Hydrogen Energy*, Vol. 32, pp. 212 – 223.

Walas, S. M., c1985, "*Phase equilibria in chemical engineering*"**,** Butterworth**,** Boston.

Wang, D., S. Czernik, D. Montane, M. Mann and E. Chornet, 1997, "Biomass to Hydrogen via Fast Pyrolysis and Catalytic Steam Reforming of the Pyrolysis Oil or Its Fractions", *Ind. Eng. Chem. Res.,* Vol. *36*, pp. 1507-1518.

Yaman, S, 2004, "Pyrolysis of biomass to produce fuels and chemical feedstocks", *Energy Conversion and Management*, Vol. 45, pp. 651–671.

Yan, Q., L. Guo and Y. L. State, 2006, "Thermodynamic analysis of hydrogen production from biomass gasification in supercritical water", *Energy Conversion and Management*, Vol. 47, pp. 1515 – 1528.

Yang, Y., J. Ma and F. Wu, 2006, "Production of hydrogen by steam reforming of ethanol over a Ni/ZnO catalyst", *International Journal of Hydrogen Energy*, Vol. 31, pp. 877–882.

"*CRC Handbook Of Data On Organic Compounds*", 1985, Crc Press, Boca Raton, Florida.